

Novel Core-Modified Expanded Porphyrins with *meso*-Aryl Substituents: Synthesis, Spectral and Structural Characterization

Seenichamy Jeyaprakash Narayanan,[†] Bashyam Sridevi,[†] Tavarekere K. Chandrashekar,^{*,‡} Ashwani Vij,[‡] and Raja Roy[§]

Contribution from the Department of Chemistry, Indian Institute of Technology, Kanpur 208016, India, Single-Crystal Diffraction Laboratory, University of Idaho, Moscow, Idaho 83843, and NMR Division, Central Drug Research Institute, Lucknow, India

Received May 4, 1999

Abstract: The synthesis, spectral and structural characterization of *meso*-aryl sapphyrins and rubyryns containing heteroatoms such as S, O, Se in addition to pyrrole nitrogens are reported. The synthesis of the desired expanded porphyrins has been achieved using a single precursor, the modified tripyrranes containing heteroatoms, through an unprecedented oxidative coupling reaction in moderately good yields. The product distribution and the isolated yields were found to be dependent on the nature of the acid catalyst and its concentration. Use of 0.1 equiv of acid exclusively gave 26π rubyryns while a higher concentration of acid gave a mixture of 18π porphyrin, 22π sapphyrin, and 26π rubyryn. Two additional products, 22π oxasmaragdyrin and 18π oxacorrole, were isolated in the reaction of oxatripyrrane. All of the sapphyrins and rubyryns exhibit well-defined intense Soret and Q-bands in the visible region, and the intensity and the position of the absorption maxima were dependent on the number and the nature of the heteroatoms present in the cavity. The solid-state structures of sapphyrins **8** and **9** show small deviations from planarity with formation of supramolecular ladders stabilized by weak C–H···S, C–H···Se, and C–H···N hydrogen bonds. ¹H NMR studies reveal retainment of supramolecular arrays in solution. The TFA adduct of **8** shows unusual binding in which both the hydroxyl oxygen and the carbonyl oxygen participate, which is reminiscent of metal carboxylate binding and in total contrast to that observed for β -substituted sapphyrins. ¹H NMR studies on rubyryns indicate rapid rotation of heterocyclic rings at room temperature, and protonation leads to a decrease in rate of rotation at room temperature. ¹H NMR spectra of **10** and **17** in its free base form recorded at -50 °C reveal that the heterocyclic rings are inverted and protonation leads to dramatic ring flipping. However, **11** shows normal structure in the solution. The single-crystal X-ray structures of **10**, **11**, and **17** show that the heterocyclic rings, thiophene in **10**, selenophene in **11**, and furan and thiophene in **17**, are inverted in the solid state.

Introduction

The recent realization that expanded porphyrins¹ have diverse applications as sensitizers for PDT,² MRI contrasting agents,³ multimetallic chelates for catalysis,⁴ receptors for anions and

neutral substrates,⁵ and media chemical sensors⁶ has led to a flurry of research activity on their synthesis, characterization, structure, and spectroscopic and electrochemical properties.⁵ They are also of interest in terms of aromaticity in large conjugated cyclic systems⁷ and the range of coordination environment available for transition metal cations.^{2a,3a,4,8} Even though the pioneering work in the sixties by Woodward^{9a} and Johnson^{9b} established the existence of expanded porphyrins, it is only in the late eighties and early nineties that the chemistry of expanded porphyrins has been exploited as a result of the advances in the syntheses of key precursors such as dipyrromethanes¹⁰ and tripyrranes^{11,12} required for the construction of the expanded porphyrin skeleton. A variety of expanded

* E-mail: tkc@iitk.ac.in. FAX: 91-512-597436/590260/590007.

[†] Indian Institute of Technology.

[‡] University of Idaho.

[§] Central Drug Research Institute.

(1) (a) Sessler, J. L.; Weghorn, S. J. *Expanded, Contracted & Isomeric Porphyrins, Tetrahedron Organic Chemistry Series, Vol. 15*; Pergamon: New York, 1997. (b) Jasat, A.; Dolphin, D. *Chem. Rev.* **1997**, *97*, 2267–2340.

(2) (a) Sessler, J. L.; Hemmi, G.; Mody, T. D.; Murai, T.; Burrell, A. K.; Young, S. W. *Acc. Chem. Res.* **1994**, *27*, 43–50. (b) Maiya, B. G.; Cyr, M.; Harriman, A.; Sessler, J. L. *J. Phys. Chem.* **1990**, *94*, 3597–3601. (c) Franck, B.; Nonn, A. *Angew. Chem. Int. Ed. Engl.* **1995**, *34*, 1795–1811. (d) Franck, B.; Fulling, M.; Gossmann, G.; Mertes, H.; Schroder, D. *Proc. SPIE-Int. Soc. Opt. Eng.* **1988**, *997*, 107–112. (e) Shiau, F.-Y.; Liddell, P. A.; Vicente, G. H.; Ramana, N. V.; Ramachandran, K.; Lee, S.-J.; Pandey, R. K.; Dougherty, T. J.; Smith, K. M. *SPIE Future Dir. Appl. Photodyn. Ther.* **1989**, *6*, 71–86. (f) Judy, M. L.; Matthews, J. L.; Newman, J. T.; Skiles, H.; Boriack, R.; Cyr, M.; Maiya, B. G.; Sessler, J. L. *Photochem. Photobiol.* **1991**, *53*, 101–107. (g) Sessler, J. L.; Hemmi, G.; Maiya, B. G.; Harriman, A.; Judy, M. L.; Boriack, R.; Matthews, J. L.; Ehrenberg, B.; Malik, Z.; Nitzan, Y.; Ruck, A. *Proc. SPIE-Int. Soc. Opt. Eng.* **1991**, *1426*, 318–329.

(3) (a) Sessler, J. L.; Murai, T.; Hemmi, G. *Inorg. Chem.* **1989**, *28*, 3390–3393. (b) Sidhu, M. K.; Muller, H. H.; Miller, R. A.; Mody, T. D.; Hemmi, G.; Sessler, J. L.; Young, S. W. *Abstracts of the 1991 National Meeting, American Association of University Radiologists, Orlando, FL, Mar 1991.*

(4) Burrell, A. K.; Sessler, J. L.; Cyr, M. J.; McGhee, E.; Ibers, J. A. *Angew. Chem., Int. Ed. Engl.* **1991**, *30*, 91–93.

(5) (a) Sessler, J. L.; Andrievsky, A.; Genge, J. W. *Adv. Supramol. Chem.* **1997**, *4*, 97–142. (b) Sessler, J. L.; Burrell, A. K.; Furuta, H.; Hemmi, G. W.; Iverson, B. L.; Kral, V.; Magda, D. J.; Mody, T. D.; Shreder, K.; Smith, D.; Weghorn, S. J. *Transition Met. Supramol. Chem.* **1994**, 391–408. (c) Sessler, J. L.; Sansom, P. I.; Andrievsky, A.; Kral, V. In *Supramolecular Chemistry of Anions*; Bianchi, A., James, K. B., Espana, E. G., Eds.; Wiley-VCH: New York, 1997; pp 355–419. (d) Shionoya, M.; Furuta, H.; Lynch, V.; Harriman, A.; Sessler, J. L. *J. Am. Chem. Soc.* **1992**, *114*, 5714–5722.

(6) Sessler, J. L.; Andrievsky, A.; Gale, P. A.; Lynch, V. *Angew. Chem., Int. Ed. Engl.* **1996**, *35*, 2782–2785.

(7) (a) Franck, B.; Nonn, A.; Fuchs, K.; Gosmann, M. *Liebigs. Ann. Chem.* **1994**, 503–510. (b) Knubel, K.; Franck, B. *Angew. Chem., Int. Ed. Engl.* **1988**, *27*, 1170–1172.

porphyrins with varying degrees of ring size, such as sapphyrins,^{9,12} pentaphyrins,¹³ hexaphyrins,¹⁴ rosarins,¹⁵ rubeprins,¹⁶ octaphyrins,¹⁷ turcasarins,¹⁸ porphocyanines¹⁹ etc., have been synthesized, and anion binding,⁵ metal chelation,^{8,4,2a,3a} and electrochemical^{5d,20} and photochemical^{20,21,2b} properties of some of them have been evaluated.

Core modification by the replacement of one or more pyrrolic units by other heterocycles such as furan, thiophene, and selenophene leads to a new class of expanded porphyrins.²² Introduction of heteroatoms into the core leads to changes in the cavity size and electronic structure, thereby altering the optical, electrochemical, and photochemical properties and could be anticipated to generate interdisciplinary interest. A perusal of literature reveals only limited reports on the synthesis and characterization of core-modified expanded porphyrins. Johnson and co-workers^{9b} reported the first synthesis of furan- and thiophene-containing sapphyrins. Later Sessler and co-workers²³ have reported a series of β -substituted sapphyrins containing

(8) (a) Sessler, J. L.; Murai, T.; Lynch, V. *Inorg. Chem.* **1989**, *28*, 1333–1341. (b) Burrell, A. K.; Hemmi, G.; Lynch, V.; Sessler, J. L. *J. Am. Chem. Soc.* **1991**, *113*, 4690–4692. (c) Sessler, J. L.; Mody, T. D.; Hemmi, G.; Lynch, V. *Inorg. Chem.* **1993**, *32*, 3175–3187. (d) Sessler, J. L.; Weghorn, S. J.; Hiseada, Y.; Lynch, V. *Chem. Eur. J.* **1995**, *1*, 56–67. (e) Sessler, J. L.; Burrell, A. K.; Lisowski, J.; Gebauer, A.; Cyr, M. J.; Lynch, V. *Bull. Chem. Soc. Fr.* **1996**, *133*, 725–734. (f) Sessler, J. L.; Gebauer, A.; Guba, A.; Scherer, M.; Lynch, V. *Inorg. Chem.* **1998**, *37*, 2073–2076.

(9) (a) Bauer, V. J.; Clive, D. L. J.; Dolphin, D.; Paine, J. B., III; Harris, F. L.; King, M. M.; Loder, J.; Wang, S. C.; Woodward, R. B. *J. Am. Chem. Soc.* **1983**, *105*, 6429–6436. (b) Broadhurst, M. J.; Grigg, R.; Johnson, A. W. *J. Chem. Soc., Perkin Trans. 1* **1972**, 2111–2116.

(10) Lee, C.-H.; Lindsey, J. S. *Tetrahedron* **1994**, *50*, 11427–11440.

(11) (a) Heo, P.-Y.; Shin, K.; Lee, C.-H. *Tetrahedron Lett.* **1996**, *37*, 197–200. (b) Bruckner, C.; Stenberg, E. D.; Boyle, R. W.; Dolphin, D. *J. Chem. Soc., Chem. Commun.* **1997**, 1689–1690. (c) Sridevi, B.; Narayanan, S. J.; Srinivasan, A.; Reddy, M. V.; Chandrashekar, T. K. *J. Porphyrins Phthalocyanines* **1998**, *2*, 69–78.

(12) Sessler, J. L.; Cyr, M. J.; Lynch, V.; McGhee, E.; Ibers, J. A. *J. Am. Chem. Soc.* **1990**, *112*, 2810–2813.

(13) Rexhausen, H.; Gossauer, A. *J. Chem. Soc., Chem. Commun.* **1983**, 275.

(14) Gossauer, A. *Bull. Soc. Chim. Belg.* **1983**, *92*, 793–795.

(15) Sessler, J. L.; Weghorn, S. J.; Morishima, T.; Rosingana, M.; Lynch, V.; Lee, V. *J. Am. Chem. Soc.* **1992**, *114*, 8306–8307.

(16) Sessler, J. L.; Morishima, T.; Lynch, V. *Angew. Chem., Int. Ed. Engl.* **1991**, *30*, 977–980.

(17) (a) Vogel, E.; Broring, M.; Fink, J.; Rosen, D.; Schmickler, H.; Lex, J.; Chan, K. W. K.; Wu, Y.-D.; Plattner, D. A.; Nendel, M.; Houk, K. N. *Angew. Chem., Int. Ed. Engl.* **1995**, *34*, 2511–2514. (b) Broring, M.; Jendry, J.; Zander, L.; Schmickler, H.; Lex, J.; Wu, Y.-D.; Plattner, D. A.; Houk, K. N.; Vogel, E. *Angew. Chem., Int. Ed. Engl.* **1995**, *34*, 2515–2517.

(18) Sessler, J. L.; Weghorn, S. J.; Lynch, V.; Johnson, M. R. *Angew. Chem., Int. Ed. Engl.* **1994**, *33*, 1509–1512.

(19) (a) Dolphin, D.; Rettig, S. J.; Tang, H.; Wijesekera, T.; Xie, L. Y. *J. Am. Chem. Soc.* **1993**, *115*, 9301–9302. (b) Dolphin, D.; Xie, L. Y. *J. Chem. Soc., Chem. Commun.* **1994**, 1475–1476. (c) Xie, L. Y.; Boyle, R. W.; Dolphin, D. *J. Am. Chem. Soc.* **1996**, *118*, 4853–4859. (d) Boyle, R. W.; Xie, L. Y.; Dolphin, D. *Tetrahedron Lett.* **1994**, *35*, 5377–5380.

(20) Maiya, B. G.; Harriman, A.; Sessler, J. L.; Hemmi, G.; Murai, T.; Mallouk, T. E. *J. Phys. Chem.* **1989**, *93*, 8111–8115.

(21) (a) Hariman, A.; Maiya, B. G.; Murai, T.; Hemmi, G.; Sessler, J. L.; Mallouk, T. E. *J. Chem. Soc., Chem. Commun.* **1989**, 314–316. (b) Levanon, H.; Regev, A.; Michaeli, S.; Galili, T.; Cyr, M.; Sessler, J. L. *Chem. Phys. Lett.* **1990**, *174*, 235–240. (c) Regev, A.; Michaeli, S.; Levanon, H.; Cyr, M.; Sessler, J. L. *J. Phys. Chem.* **1991**, *95*, 9121–9129. (d) Bachmann, R.; Gerson, F.; Putz, C.; Vogel, E. *J. Chem. Soc., Perkin Trans. 2* **1996**, 541–546. (e) Srinivasan, A.; Kumar, M. R.; Pandian, R. P.; Mahajan, S.; Pushpan, K. S.; Sridevi, B.; Narayanan, S. J.; Chandrashekar, T. K. *J. Porphyrins Phthalocyanines* **1998**, *2*, 1–10.

(22) (a) Ravikanth, M.; Chandrashekar, T. K. *Struct. Bonding (Berlin)* **1995**, *82*, 105–188. (b) Gouterman, M. In *The Porphyrins*; Dolphin, D., Ed.; Academic Press: New York, 1978; Vol. III, pp 1–165.

(23) (a) Sessler, J. L.; Cyr, M.; Burrell, A. K. *Tetrahedron* **1992**, *48*, 9661–9672. (b) Lisowski, J.; Sessler, J. L.; Lynch, V. *Inorg. Chem.* **1995**, *34*, 3567–3572. (c) Sessler, J. L.; Gebauer, A.; Hoehner, M. C.; Lynch, V. *J. Chem. Soc., Chem. Commun.* **1998**, 1835–1836. (d) Sessler, J. L.; Hoehner, M. C.; Gebauer, A.; Andrievsky, A.; Lynch, V. *J. Org. Chem.* **1997**, *62*, 9251–9260.

one or more heteroatoms. Ibers and co-workers²⁴ have reported the synthesis of oxabronzaphyrin, thiazaphyrin, and a thiophene-containing porphycene-like 26π macrocycle by McMurray coupling of appropriate dialdehydes. Cava et al.²⁵ have synthesized thiophene- and furan-containing annulenes, and Vogel and co-workers²⁶ have recently reported the synthesis of sulfur- and selenium-containing pentaphyrins. There are few reports on furan-containing 22π and 26π expanded macrocycles.²⁷ Very recently Lash and co-workers²⁸ reported the synthesis of carbasapphyrins by a [4 + 1] reaction of tetrapyrrole with dialdehyde. Interestingly, in most of the above examples, the expanded porphyrins have β -pyrrole substituents but free meso carbon bridges.

Surprisingly, reports on the synthesis of expanded porphyrins bearing *meso*-aryl substituents are very few and have appeared very recently. Latos-Grazynski and co-workers²⁹ were the first to isolate N-5 *meso*-aryl sapphyrin as a byproduct in Rothmund reaction in 1.1% yield. Later, Dolphin and co-workers^{5b} described a rational synthesis of N-5 *meso*-aryl sapphyrins using tripyrranes in about 30% yield. Synthesis of diaryl sapphyrins in 9.5% yield was reported by Sessler and co-workers^{30a} under Lindsey conditions^{30b} using bipyrrrole dialdehyde, pyrrole, and benzaldehyde. We have been interested in the synthesis of core-modified expanded porphyrins, and recent work from this laboratory has described the synthesis of a series of heteroatom sapphyrins and rubeprins in moderately good yields.³¹ Most of the synthetic methodology described above require at least two sensitive precursors, which involves a multistep synthesis before the final condensation step, thus restricting the yield of the final product. Furthermore, development of easy and efficient methodology to synthesize the expanded porphyrins in multigram quantities is still a synthetic challenge to exploit their diverse applications. In this paper, we wish to report the synthesis, characterization, and X-ray crystal structures of a series of 22π sapphyrins and 26π rubeprins using a single precursor by an unprecedented oxidative coupling reaction. It has been shown that by choosing appropriate reaction conditions, it is possible to control the product distribution and yield. Furthermore, the structure of sapphyrins reveals the formation of supramolecular

(24) (a) Miller, D. C.; Johnson, M. R.; Becker, J. J.; Ibers, J. A. *J. Heterocycl. Chem.* **1993**, *30*, 1485–1490. (b) Johnson, M. R.; Miller, D. C.; Bush, K.; Becker, J. J.; Ibers, J. A. *J. Org. Chem.* **1992**, *57*, 4414–4417. (c) Miller, D. C.; Johnson, M. R.; Ibers, J. A. *J. Org. Chem.* **1994**, *59*, 2877–2879.

(25) (a) Hu, Z.; Kelley, C. S.; Cava, M. P. *Tetrahedron Lett.* **1993**, *34*, 1879–1882. (b) Hu, Z.; Atwood, J. L.; Cava, M. P. *J. Org. Chem.* **1994**, *59*, 8071–8075.

(26) (a) Vogel, E.; Pohl, M.; Herrmann, A.; Wiss, T.; König, C.; Lex, J.; Gross, M.; Gisselbrecht, J. P. *Angew. Chem., Int. Ed. Engl.* **1996**, *35*, 1520–1524. (b) Vogel, E.; Frode, C.; Breihan, A.; Schmickler, H.; Lex, J. *Angew. Chem., Int. Ed. Engl.* **1997**, *36*, 2609–2612.

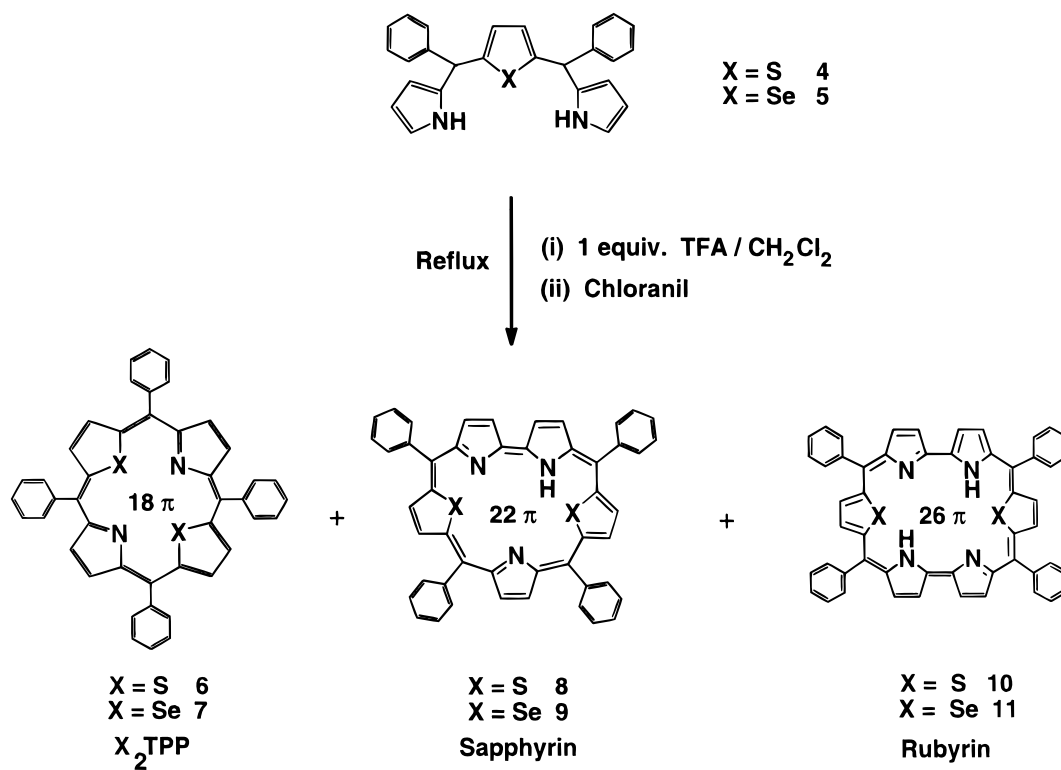
(27) (a) Markl, G.; Striebl, U. *Angew. Chem., Int. Ed. Engl.* **1993**, *32*, 1333–1355. (b) Markl, G.; Sauer, H.; Kreitmeyer, P.; Burgemeister, T.; Kastner, F.; Adolin, G.; Noth, H.; Polborn, K. *Angew. Chem., Int. Ed. Engl.* **1994**, *33*, 1151–1153. (c) Vogel, E. *Pure Appl. Chem.* **1993**, *65*, 143. (d) Markl, G.; Striebl, U.; Knorr, A.; Porsch, M.; Daub, J. *Tetrahedron Lett.* **1995**, *36*, 4401. (e) Markl, G.; Knott, T.; Kreitmeyer, P.; Burgemeister, T.; Kastner, F. *Tetrahedron* **1996**, *52*, 11763.

(28) Lash, T. D.; Richter, D. T. *J. Am. Chem. Soc.* **1998**, *120*, 9965–9966.

(29) Latos-Grazynski, L.; Rachlewicz, K. *Chem. Eur. J.* **1995**, *1*, 68–72.

(30) (a) Sessler, J. L.; Lisowski, J.; Boudreaux, K. A.; Lynch, V.; Barry, J.; Kodadek, T. J. *J. Org. Chem.* **1995**, *60*, 5975–5978. (b) Lindsey, J. S.; Schreiman, I. C.; Hsu, H. C.; Kearney, P. E.; Marguerettaz, A. M. *J. Org. Chem.* **1987**, *52*, 827–836.

(31) (a) Srinivasan, A.; Reddy, M. V.; Narayanan, S. J.; Sridevi, B.; Pushpan, S. K.; Kumar, M. R.; Chandrashekar, T. K. *Angew. Chem., Int. Ed. Engl.* **1997**, *36*, 2598–2601. (b) Srinivasan, A.; Mahajan, S.; Pushpan, S. K.; Kumar, M. R.; Chandrashekar, T. K. *Tetrahedron Lett.* **1998**, *39*, 1961–1964. (c) Pushpan, S. K.; Narayanan, S. J.; Srinivasan, A.; Mahajan, S.; Chandrashekar, T. K.; Roy, R. *Tetrahedron Lett.* **1998**, *39*, 9249–9252.

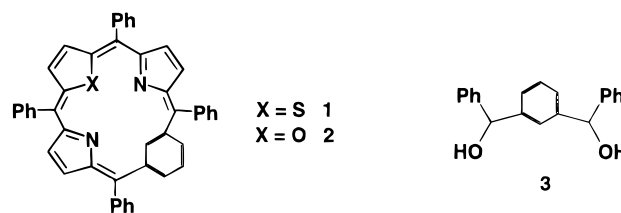
Scheme 1. Synthesis of Core-Modified Macrocycles Containing Sulfur and Selenium

ladders stabilized by weak C–H···S and C–H···Se hydrogen-bonding interactions, and such interactions are disrupted upon protonation with TFA. The structure of the TFA adducts indicate unusual binding in which both the carboxy oxygen and the hydroxy oxygen bind through H-bonding with the protons of the pyrrole nitrogens. The rubyrins also show unusual structures in solid state where the two heterocyclic rings which are linked to bipyrrrole units are inverted, in contrast to a β -substituted structure of N-6 rubyrin hydrochloride salt.¹⁶ A preliminary report on this work has appeared recently.³²

Results and Discussion

Irrespective of the nature of the expanded porphyrin, the currently available methods make use of an acid-catalyzed [3 + 2],^{9,12} [4 + 2],¹⁶ [3 + 3],^{11,8d} or [4 + 1]²⁸ condensation between the appropriate precursors, tripyrranes, terpyrranes, tetrapyranes, and the diformylbipyrroles, or the acid-catalyzed cyclo condensation of 2-hydroxy-methyl pyrroles and their analogues.^{33,7} More recently Smith and co-workers^{34a} synthesized sapphyrins by an acid-catalyzed condensation of *a,c*-biladienes with pyrrole-2-carboxaldehyde. Recent work from this laboratory made use of the reaction of bithiophene or bifuran diols with either pyrrole or dipyrromethane to synthesize core-modified sapphyrins and rubyrins in moderately good yields.³¹ In an attempt to synthesize **1** or **2** through an acid-catalyzed [3 + 1] condensation of **4** or **12** with **3** and subsequent oxidation with chloranil, we were surprised to discover the formation of 18 π X₂TPP, 22 π sapphyrin, and 26 π rubyrin in the reaction mixture. Subsequent reaction of **4** under identical conditions without the addition of **3** also resulted in the formation of **6**, **8**,

and **10** (Scheme 1). Change of acid from TFA to TsOH also gave the same products, and the product distribution and yields



were found to be dependent on the concentration of the acid catalyst. For example, reaction of **5** at 0.1 equiv of TFA exclusively gave **11** in 10.6% yield, whereas reaction at 2 equiv of TFA gave **9** (9.2%), **11** (18.3%), and **7** (1%). Chart 1A summarizes the isolated yields of various products under different acid concentrations. In general, in reaction of tripyrranes containing S or Se, at 0.1 equiv of TFA, only 26 π rubyrins were formed, whereas at higher concentrations of TFA both rubyrins and sapphyrins were formed in addition to 18 π modified porphyrins. The formation of rubyrins at lower concentration clearly suggests an unprecedented self-coupling of the tripyrranes, with the formation of two pyrrole–pyrrole links at the final condensation step.

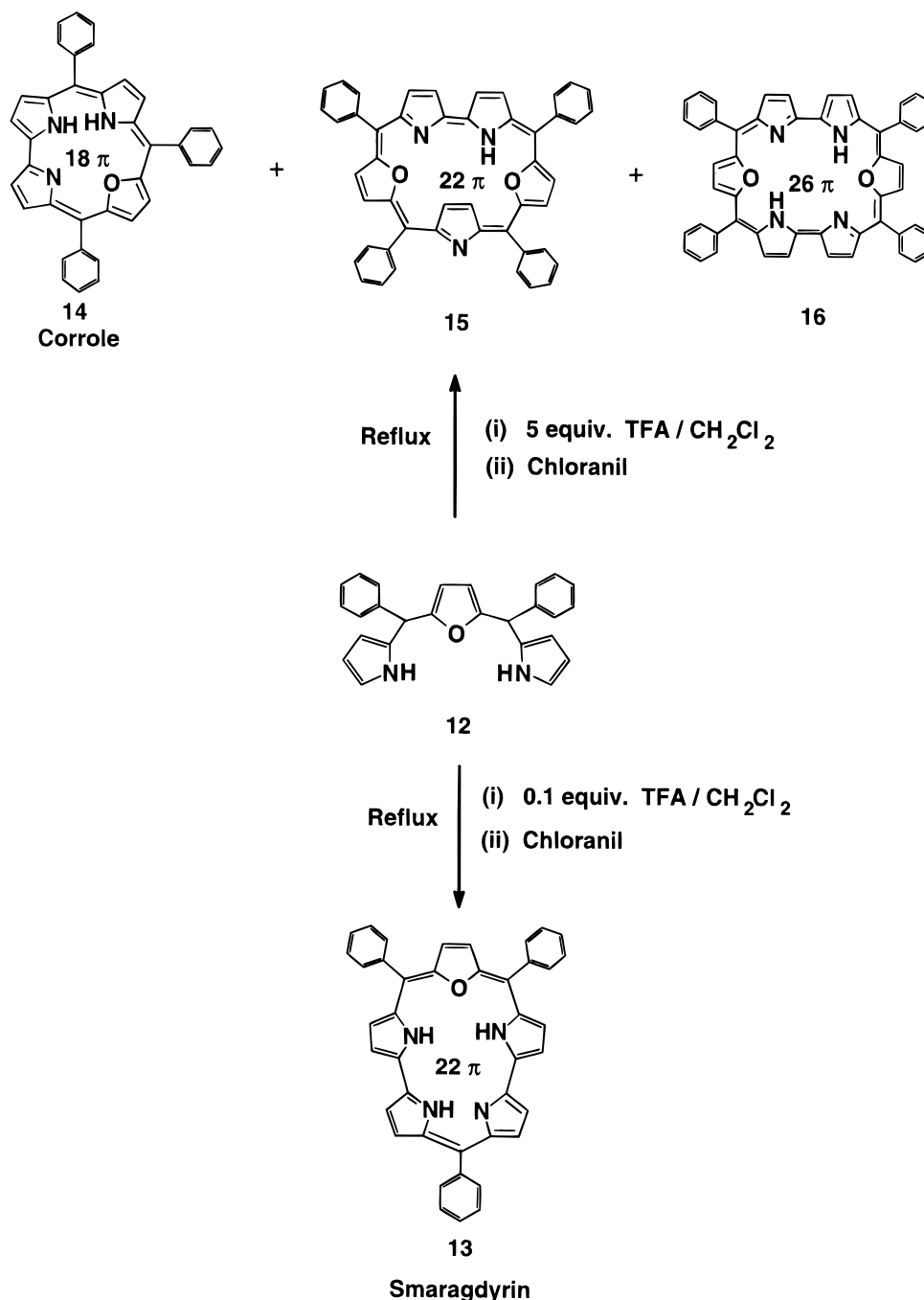
In contrast, oxatripyrrane **12** gave different products at different concentrations of TFA (Scheme 2). Compound **13** was isolated as the sole product (3.5%) in addition to some polymeric materials at 0.1 equiv of TFA, whereas at higher concentrations of TFA, in addition to **15** and **16**, the ring-contracted oxacorrole **14** was also isolated (Chart 1B). Trace amounts of O₂TPP were also formed at higher concentrations. Compound **13** was found to be relatively stable for extended periods under nitrogen and vacuum without any noticeable decomposition.

The observation that the rubyrins are exclusively formed at low concentrations of TFA led us to attempt a mixed condensation of two different tripyrranes to get the rubyrins with two

(32) Narayanan, S. J.; Sridevi, B.; Chandrashekar, T. K.; Vij, A.; Roy, R. *Angew. Chem., Int. Ed. Engl.* **1998**, *37*, 3394–3397.

(33) Gosmann, M.; Franck, B. *Angew. Chem., Int. Ed. Engl.* **1986**, *25*, 1100–1101.

(34) (a) Paolesse, R.; Licocchia, S.; Spagnoli, M.; Boschi, T.; Khoury, R. G.; Smith, K. M. *J. Org. Chem.* **1997**, *62*, 5133–5137. (b) Licocchia, S.; Vona, M. L.; Paolesse, R. *J. Org. Chem.* **1998**, *63*, 3190–3195.

Scheme 2. Synthesis of Core-Modified Macrocycles Containing Furan

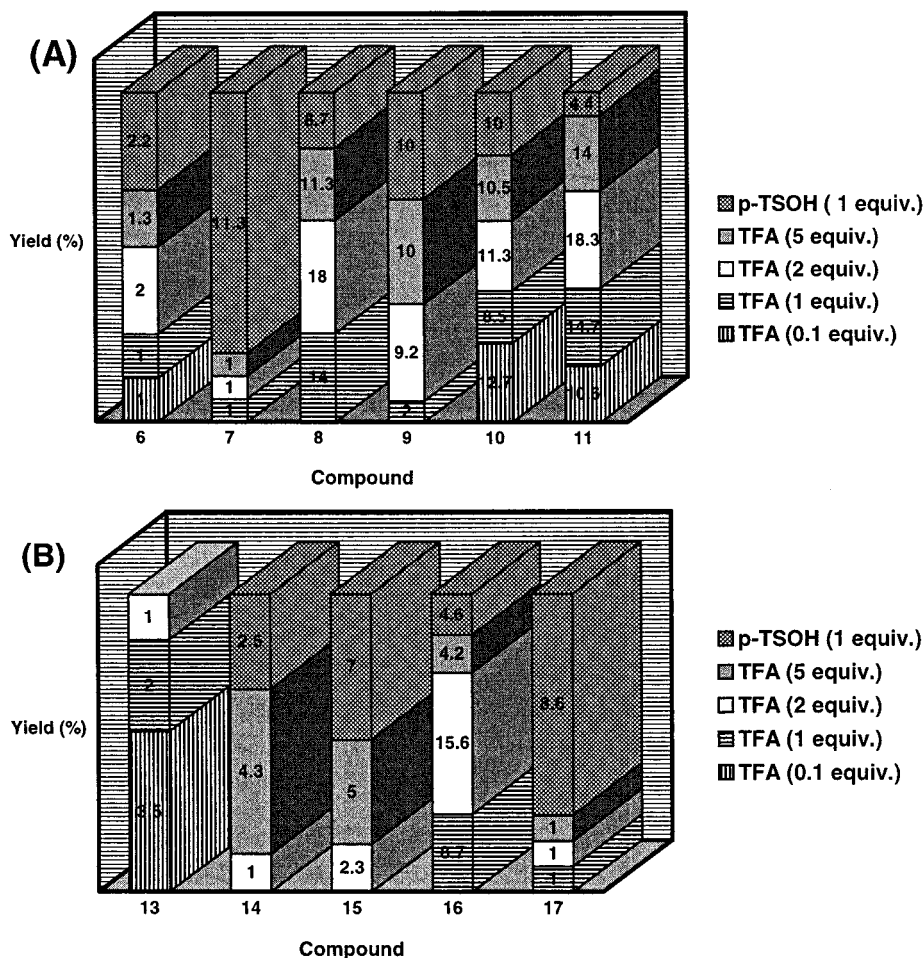
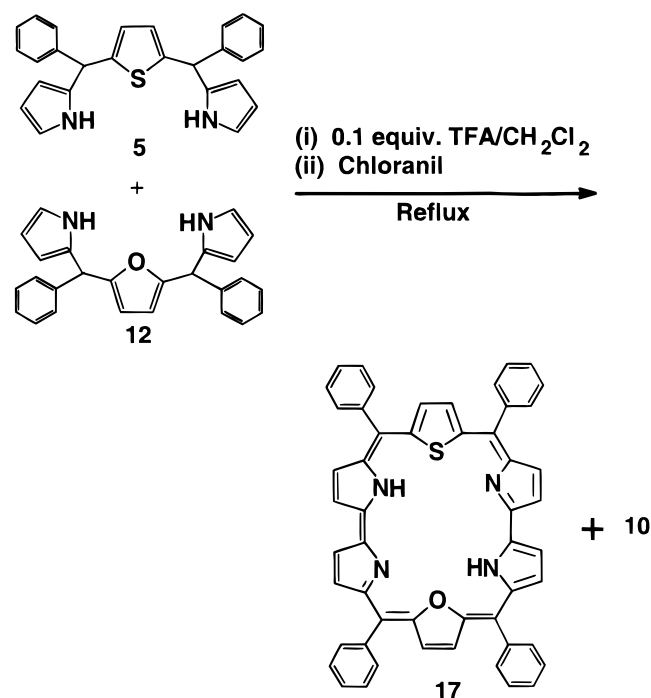
different heteroatoms (Scheme 3). Thus, condensation of **5** and **12** at 0.1 equiv of TFA followed by oxidation gave **17** in 25% yield in addition to **10** (2.8% yield).

The sole formation of rubyrins at lower TFA concentrations indicates an α - α self-coupling of the tripyrranes with the formation of two direct pyrrole-pyrrole links to form a rubyrinogen type intermediate,²⁹ which on subsequent oxidation with chloranil yields the 26 π macrocycle (Scheme 4). The protonation of tripyrrane leads to the two intermediates I and II in which protonation occurs at α and β positions, respectively. We choose to prefer the reaction of intermediate II (being the active species) through an intermolecular electrophilic attack to form intermediate III.^{34b} Further rearrangement of III followed by oxidation of chloranil results in the formation of rubyrins. Attempts to isolate these intermediates proved futile as a result of its instability toward oxidation to the aromatic congener. This

method of making rubyrin is easy and efficient relative to the literature method¹⁶ in which at least two precursors involving multistep syntheses are required before the final condensation step. Also, in Sessler's method,^{12,30} the precursors contained preformed pyrrole-pyrrole links, whereas in the present method, this pyrrole-pyrrole link is formed at the last stage, as is the case for the corroles and sapphyrins reported by Smith *et al.*³⁴

The formation of sapphyrins and porphyrins in the reaction at higher concentrations of acid catalyst require fragmentation of the tripyrranes followed by condensation of the fragmented products.³⁵ Spectrophotometric and TLC analysis of the reaction mixtures provides satisfactory evidence for the fragmentation. Specifically, reaction of oxatripyrrane with 5 equiv of TFA resulted in the appearance of weak band at 485 nm within 10

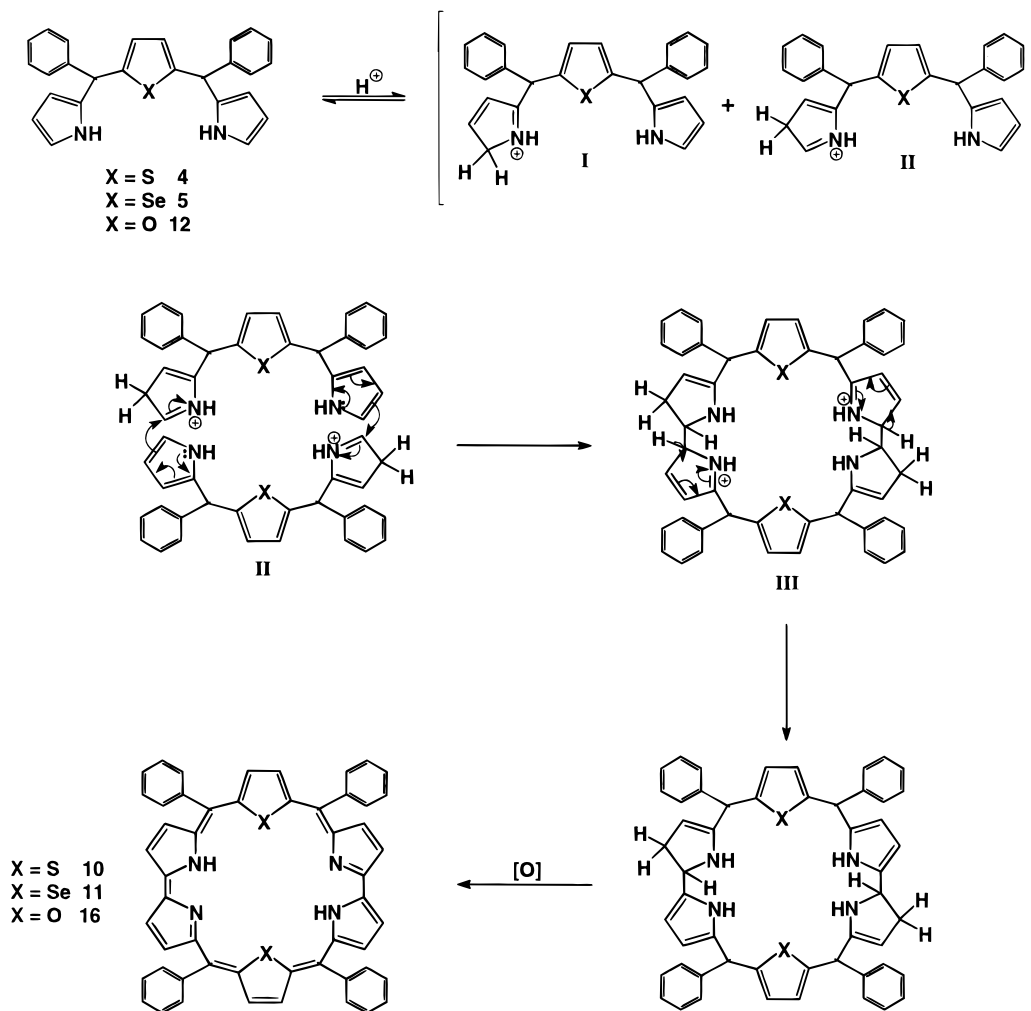
(35) Lash, T. D.; Chaney, S. T.; Richter, D. T. *J. Org. Chem.* **1998**, *63*, 9076-9088 and references therein.

Chart 1. Graphical Representation for the Yields of Macrocycles Obtained in Coupling Reactions: (A) Yield Data for Sulfur- and Selenium-Containing Macrocycles and (B) Yield Data for Oxygen-Containing Macrocycles**Scheme 3.** Synthesis of Rubyrin Having Oxygen and Sulfur in the Core

min of addition of TFA. The intensity was found to be increasing with time, and the maximum absorption was attained after 75

min of addition. We attribute this to the formation of an uncyclized conjugated macrocycle. Addition of chloranil resulted in the appearance of intense bands around 450–500 nm and weak bands in the range of 600–900 nm, suggesting the formation of the expanded porphyrins. Furthermore, the TLC analysis of tripyrrane after addition of TFA reveals additional purple to red colored spots above and below the spot of tripyrrane, and the intensity of the spots depends on the acid concentration present at that time. Addition of chloranil results in complete disappearance of the tripyrrane spot with new dark spots suggesting the formation of macrocycles. The tripyrrane fragments undergo acid-catalyzed cyclization to give sapphyrins and porphyrins. Very recently, Lash and co-workers³⁵ have reported that the β -substituted tripyrranes undergo fragmentation in the presence of acid catalyst and suggested the formation of pyrrole and dipyrromethane in the reaction mixture. The possible fragmented products in modified tripyrranes reported here could be diol, heteroatom-containing dipyrromethane, and pyrrole in addition to the unfragmented tripyrrane.³⁵ If this is true, then one would anticipate that the reaction of pyrrole and diols containing heteroatoms under appropriate conditions should give a mixture of expanded porphyrins. Indeed, independent work from this laboratory^{31c} and from the laboratory of Latos-Grazynski³⁶ has shown that it is possible to synthesize expanded porphyrins by simple reaction of diols and pyrrole. The formation of **13** and **14**³⁷ from the reaction of oxatripyrrane is interesting considering the fact that smaragdyrins are reported

(36) Rachlewicz, K.; Sprutta, N.; Chmielewski, P. J.; Latos-Grazynski, L. *J. Chem. Soc., Perkin Trans 2* **1998**, 969–975.

Scheme 4. Possible Mechanism for the Formation of Rubyrins

to be highly unstable toward acid and light. However, to our surprise, **13** is very stable and even forms metal complexes with transition metals. The preliminary X-ray structure of the Rh(I) complex of **13** indicates that only one imino and one amino nitrogen participate in coordination with the metal. Even **14** form stable metal complexes with Ni(II), Cu(II), Co(II), and Rh(I).³⁸

The disadvantage of the methodology described here is the formation of a mixture of products in the reaction. Fortunately, the ease of separation of the products due to their differing polarity, moderately good yields, and the easy synthesis of the only precursor in yields more than 60% makes the methodology efficient and effective.

Spectral Characterization. The new expanded porphyrins were characterized by FAB-MS, UV-vis, proton 1D and 2D NMR, and single-crystal X-ray crystallography. FAB-MS conforms to the proposed composition. The UV-vis spectra show an intense Soret-like band in the region 440–550 nm with ϵ values of the order $10^5 \text{ mol}^{-1} \text{ cm}^{-1}$ and Q-type absorptions in the region of 550–1100 nm. Representative UV-vis spectra

(37) X-ray structures of both **13** and **14** have been solved. **13** shows a nonplanar structure (N2 -0.0171, N3 -0.0041, N1 0.0145, N4 0.0120 Å) with a *P1* space group. There are two crystallographically independent molecules in the unit cell. **14** shows a nearly planar structure (N1 0.0155, N2 -0.0039, N3 -0.0046, O1 -0.0051 Å) with small deviations. The structural details will be published separately.

(38) Compound **14** behaves differently with respect to coordination towards transition metals. For example, the X-ray structure of the Ni(II) complex shows coordination of all three pyrrole nitrogens and the furan oxygen, while in the Rh(I) complex, only one amino and one imino nitrogen are coordinated. The details of the structure will be published separately.

of the free base of **9** and the protonated derivative of **16** shown in Figure 1a and 1b, respectively, clearly establish the porphyrinic nature of the macrocycles.^{22b} The gradual red shift of the absorption bands and the linear relationship (Figure 1c) between the number of π electrons and the wavelength of the most intense absorption band (Soret) are consistent with the increased delocalization pathway on the expansion of the ring.^{2c} A comparison of ϵ values for the dications described here with those reported by Franck and co-workers shows that the ϵ values are smaller by an order of 10 relative to those of the 22π and 26π macrocycles of Franck *et al.*^{2c}

The aromatic nature of the macrocycles was established from the observed $\Delta\delta$ values^{2c} (the difference in chemical shift of the inner NH protons and the outer ring protons in the ¹H NMR spectrum), which is a measure of the size of the ring current. The $\Delta\delta$ values vary in the range 11.78–14.87 for the various macrocycles reported in this work, and they compare well to those observed for N-5 *meso*-aryl saphyrin (14.8)¹² and N-6 rubyrin (16.5).¹⁶ However, these values are much smaller than those observed for 22π [20.2 (from inner CH and outer CH) and 19.39 (from inner NH and outer CH)] and 26π [24.1 (from inner CH and outer CH) and 20.12 (from inner NH and outer CH)] macrocycles of Franck^{2c} as a result of the nonplanar structure of macrocycles (*vide infra*).

N-H Tautomerism in Sapphyrins. Unlike β -substituted sapphyrins, the *meso*-aryl sapphyrins exhibit two types of geometry referred to as planar and inverted.³⁹ In the planar geometry, the pyrrole nitrogen atom in the ring opposite to the

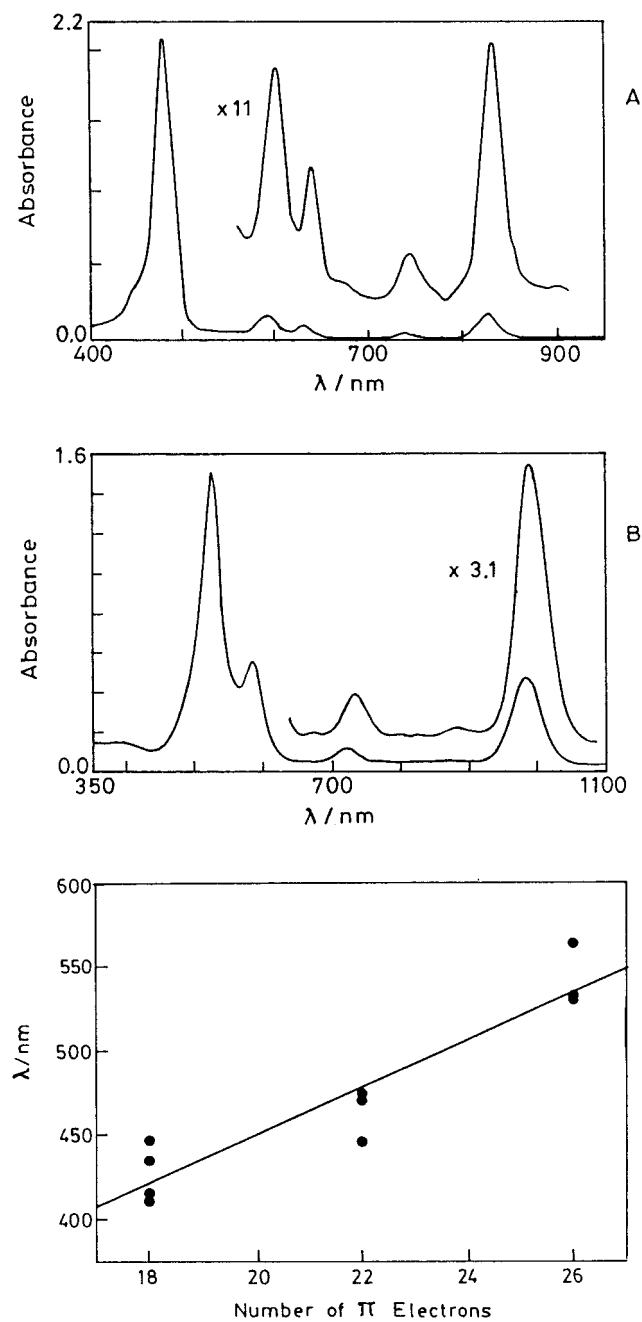


Figure 1. (A) UV-vis spectra for **9** (6.976×10^{-6} M) in dichloromethane, (B) UV-vis spectra for diprotonated salt of **16** (1.807×10^{-5} M) in dichloromethane with excess TFA solution, and (C) plot of number of π electrons versus λ_{\max} of the core-modified expanded porphyrins.

bipyrrole unit is in the ring current region while the β protons of the ring are in the periphery; in the inverted geometry, the heteroatom is in the periphery while the β -CH protons come into the ring current region. The ^1H NMR chemical shifts can easily distinguish between the two geometries. The N-5 *meso*-aryl sapphyrin show an inverted geometry in its free base form and planar geometry when it is protonated.^{39,40} Thus ^1H NMR chemical shifts of **8**, **9**, and **15** suggest that **8** and **9** have planar structures while **15** has inverted structure.³⁶ Unlike in N-5 *meso*-

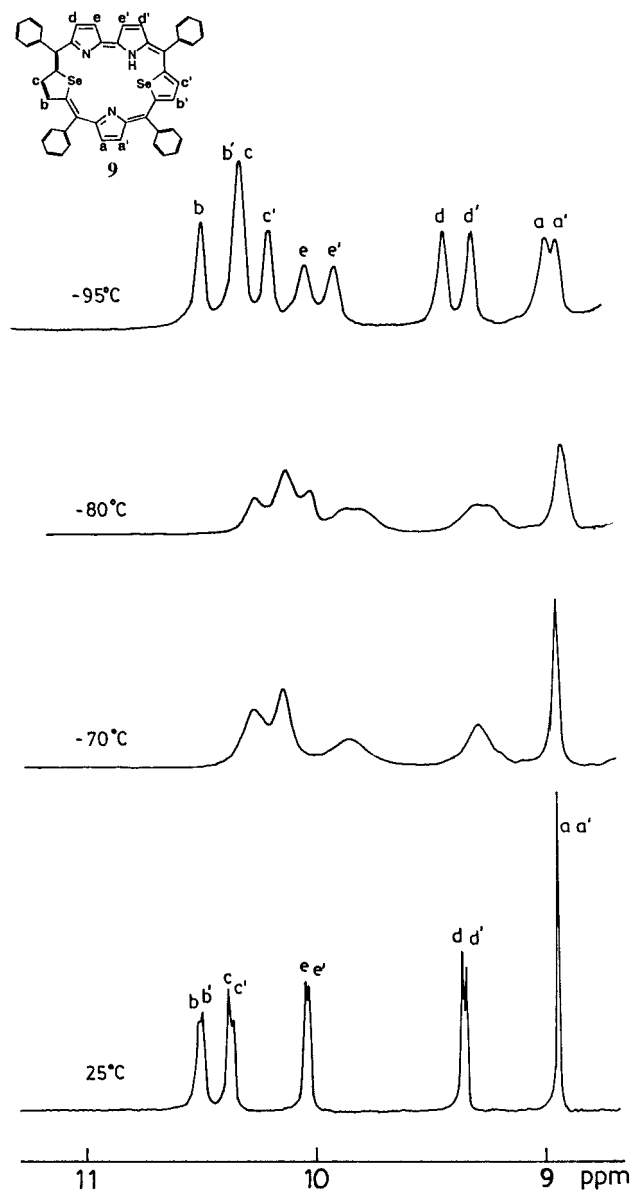


Figure 2. ^1H NMR spectra of **9** at variable temperatures in CD_2Cl_2 .

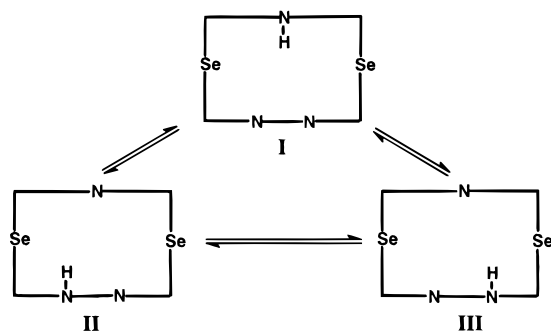
aryl sapphyrin **8**, **9** and **15** do not show any ring flipping upon protonation.

The ^1H NMR spectra of **8** and **9** reveal that the NH tautomerism in **8** is rapid relative to that in **9** at room temperature, resulting in the appearance of a broad signal at -4.4 ppm for **9** while no signal is observed for **8** for the inner NH proton. However, on cooling of the solution to -95 °C, sharp resonances are seen for both **8** and **9** at -5.0 and -5.35 ppm, respectively. Significant changes are observed in the aromatic region upon variation of temperature from 25 to -95 °C (Figure 2). Specifically, in addition to line broadening of all of the resonances, the selenophene protons (bb' , cc'), bipyrrole protons (dd' , ee'), and pyrrole protons (aa') that were equivalent at 25 °C show doubling of peaks at -95 °C. This observation can be explained by assuming the following possible tautomeric equilibrium. The equivalence of pyrrole, selenophene, and bipyrrole protons at room temperature suggests the existence of a rapid tautomerism, as observed for many tetrapyrrolic macrocycles.⁴¹ However, at -95 °C, the existence of tautomer I is excluded by the fact that this is a symmetric tautomer with respect to the mirror plane passing through the pyrrole nitrogen and the middle of bipyrrolic unit and accordingly only a singlet

(39) Rachlewicz, K.; Sprutta, N.; Latos-Grazynski, L.; Chmielewski, P. J.; Sztrenberg, L. *J. Chem. Soc., Perkin Trans 2* **1998**, 959–967.

(40) Narayanan, S. J.; Sridevi, B.; Srinivasan, A.; Chandrashekar, T. K.; Roy, R. *Tetrahedron Lett.* **1998**, 39, 7389–7392.

is expected for the pyrrole protons (aa') at this temperature, in contrast to experimental observation. Furthermore, the doubling of the selenophene protons (bb', cc') and bipyrrrole protons (dd',



ee') suggests that the proton is exchanging site only between two bipyrrrolic nitrogens, revealing the existence of tautomers of II and III. A similar observation was made by Latos Grazynski et al.³⁶ for **8** and **15** very recently, and activation parameters are also reported. Upon protonation two separate NH resonances are seen for **8** and **9**, suggesting the inequivalence of pyrrole and bipyrrrole NH protons, as well as retainment of planar geometry.

¹H NMR spectral studies of **13** and **14** also show considerable aromatic character despite the removal of a meso carbon. The NH tautomerism in **13** is very rapid, and even at $-50\text{ }^{\circ}\text{C}$ the inner NH resonances are not seen in the NMR spectrum, suggesting that the molecule adopts a symmetric conformation with respect to the mirror plane passing through the methine bridge and the furan oxygen atom. The bipyrrrole protons and the furan protons resonate in the aromatic region. In contrast, **14** exhibits asymmetric tautomerism in which the NH proton adjacent to the furan ring is localized and only the NH proton on the bipyrrrole ring is changing sites between the two nitrogen atoms of the bipyrrrole ring. This observation was confirmed by the 2D-TOCSY spectrum.

Structure of Sapphyrins. In accordance with ¹H NMR results, both **8** and **9** show a planar structure in the solid state, with only small deviations from the planarity.³² Substitution of pyrrole NH by S and Se changes the π electron delocalization pattern, and the bond distances are altered in the macrocycles relative to the free thiophene or selenophene rings. The NH proton present on the bipyrrrole nitrogen shows hydrogen bonding interactions with both of the heteroatoms inside the cavity. For example, H \cdots S1 and H \cdots S2 distances for **8** are 2.87(8) Å and 2.55(8) Å, whereas the corresponding H \cdots Se1 and H \cdots Se2 distances for **9** are 2.63(17) Å and 2.28(17) Å, respectively. The important feature of the structure is the presence of weak intermolecular hydrogen-bonding interactions involving C–H \cdots S and C–H \cdots Se in **8** and **9**, respectively; as described previously,³² these interactions are responsible for the supramolecular ladder-like arrangement of **8** and **9** in the solid state.

To investigate whether these supramolecular structures are confined only to solid-state packing forces or they are prevalent in solution, we have recorded ¹H NMR spectra of crystals of **9** grown in two different solvent mixtures. To our surprise, the crystals grown in a CH₂Cl₂/CH₃OH mixture (the one used for

X-ray analysis) show broad resonances of varying line widths (20.1, 18.1, and 12 Hz). However, the crystals grown in a CH₂Cl₂/hexane mixture show sharp well-defined resonances for the pyrrole, bipyrrrole, selenophene, and meso phenyl protons. Figure 3 shows the effect of addition of different concentrations of methanol to the solution containing a crystal of **9** grown in the CH₂Cl₂/hexane mixture. It is seen from the figure that addition of methanol results in line broadening of pyrrole protons (a), selenophene protons (b, c), bipyrrrole protons (d, e), and phenyl protons (f–i) and that the extent of broadening is different for different protons. Furthermore, the spectrum of the crystal grown in CH₂Cl₂/CH₃OH (the one used for X-ray analysis) resembles that shown in Figure 3 after addition of methanol. This observation clearly suggests that supramolecular array is retained in solution as well.⁶ Compound **8** also behaves in the same fashion.

The structure of the TFA adduct of **8** is shown in Figure 4. There are five TFA molecules in the unit cell, out of which only one is directly involved in binding with the protons of the ring nitrogens above the plane of the macrocycle. The second TFA molecule is linked to bound TFA through O7 with O7 \cdots H–O hydrogen bonding (length 2.571(14) Å, bond angle 170.62 $^{\circ}$). The remaining TFA molecules are linked with each other through a series of O \cdots H–O hydrogen bonds and are linked to the sapphyrin molecule by C19–H19A \cdots F1 (3.17(3) Å, 129.02 $^{\circ}$), C39–H39 \cdots O5 (3.374(10) Å, 168.15 $^{\circ}$), and C44–H44A \cdots O5 (3.483(10) Å, 174.30 $^{\circ}$). The TFA binding results in severe nonplanarity of the otherwise planar macrocycle, in which the two thiophene rings are twisted below the plane of the macrocycle. The three nitrogen atoms bearing protons that are involved in binding are pointing above the plane of the macrocycle, facilitating the binding of the anion.

Sessler and co-workers^{23d} have recently published solid state structures of TFA adducts of two sapphyrins, all aza sapphyrins (N5) and a furan-containing sapphyrin (ON4), in which two molecules of TFA are bound above and below the plane of the macrocycle. We choose to compare the mode of binding of TFA in N5 and ON4 sapphyrins with the TFA adduct of **8**. This comparison, shown in Scheme 5, reveals many interesting similarities and differences: (a) In both N-5 and ON4 sapphyrins, two molecules of TFA are bound, one each above and below the plane of the macrocycle, with N–H \cdots O interactions. One TFA has three such interactions in both the cases, while the other in N-5 has two and ON4 has one such interaction, corresponding to the number of available hydrogen bonding sites.^{23d} (b) In both cases, the carbonyl oxygen is not involved in binding. (c) In the TFA adduct of **8** only one TFA molecule is involved in direct binding with the macrocycle with three N–H \cdots O interactions, but the difference is that both of the oxygens of TFA are involved in the binding, which is reminiscent of metal carboxylate binding in metal complexes.⁴² The C–O distances are almost similar (C1_c–O7, 1.233(7) Å and C1_c–O8, 1.238(7) Å). These CO bond distances and the OCO bond angle (O7–C1_c–O8, 128.0(6) $^{\circ}$) compare well with the copper complex of trifluoro carboxylate (C–O, 1.242(11) Å and O–C–O 129.0(9) $^{\circ}$).⁴² (d) A comparison of the bond distances listed show a regular decrease in the N–H \cdots O bond length as the number of such interactions are reduced. This comparative data clearly highlights how the macrocycle adjusts itself to the environment (in this case, a reduced number of H-bonding sites) around which it should bind anions.

¹H NMR of Rubyrins. The ¹H NMR spectra of rubyrins are found to be critically dependent on the temperature. At room

(42) Doedens, R. J. *Progress in Inorganic Chemistry*; Lippard, S. J., Ed.; John Wiley & Sons: New York, 1976; 21, pp 209–231.

(41) (a) Crossley, M. J.; Field, L. D.; Harding, M. M.; Sternhell, S. *J. Am. Chem. Soc.* **1987**, *109*, 2335–2341. (b) Vogel, E.; Kocher, M.; Schmickler, H.; Lex, J. *Angew. Chem., Int. Ed. Engl.* **1986**, *25*, 257–259. (c) Wehrle, B.; Limbach, H.-H.; Kocher, M.; Ermer, O.; Vogel, E. *Angew. Chem., Int. Ed. Engl.* **1987**, *26*, 934–936. (d) Braun, J.; Schlabach, M.; Wehrle, B.; Kocher, M.; Vogel, E.; Limbach, H.-H. *J. Am. Chem. Soc.* **1994**, *116*, 6593–6604.

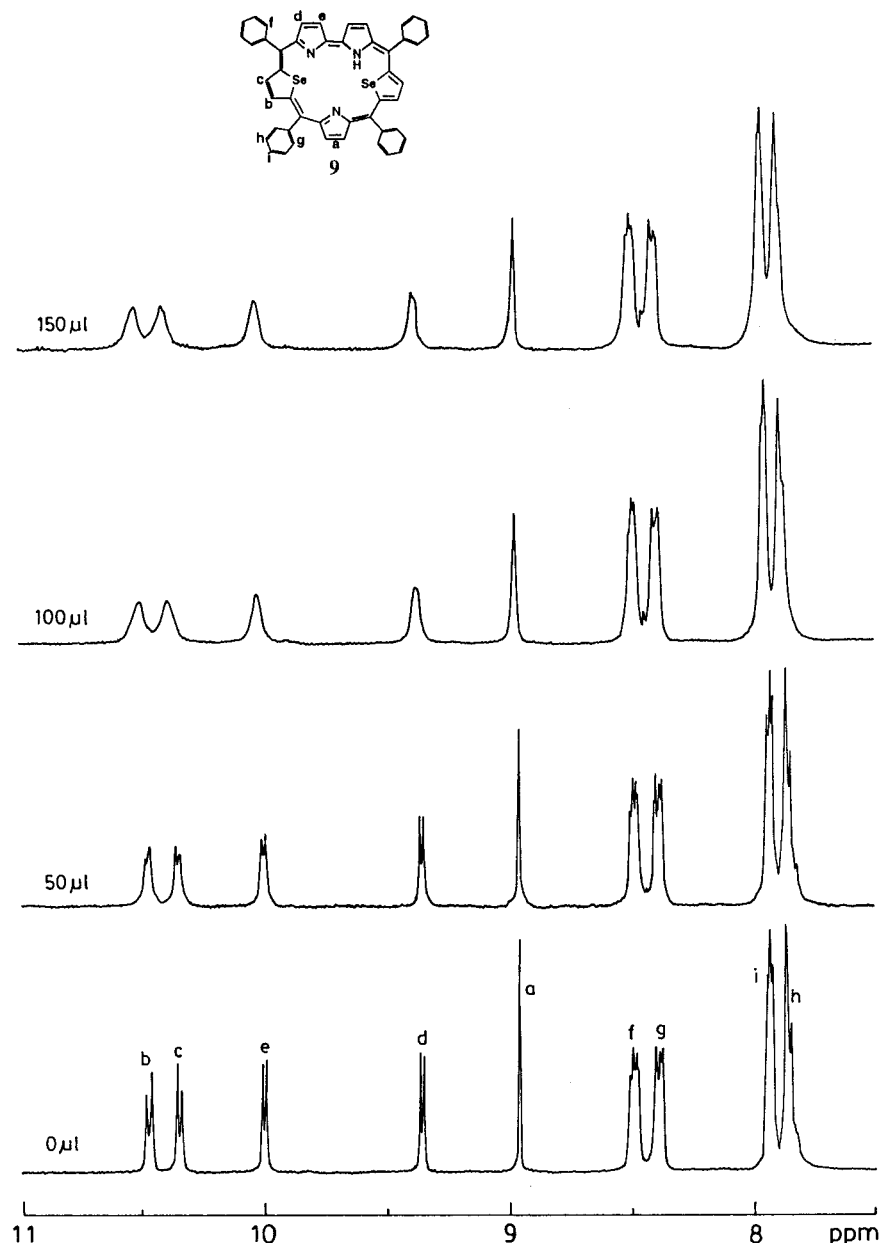


Figure 3. Effect of the addition of different concentrations of methanol on the ^1H NMR spectra of **9** ($4.94 \times 10^{-3}\text{M}$). The number on the left (μL) represents the concentration of methanol added.

temperature all of the rubeans give only broad signals (line width, ~ 38.4 Hz), and as the temperature is lowered the spectrum becomes fairly resolved, making assignments possible. This observation suggests that the heterocyclic rings linked to the bipyrrrole units are rapidly rotating and at low temperature the rate of rotation is reduced relative to the NMR time scale. It is also observed that protonation of the rubeans leads to reasonably resolved spectra, suggesting that the protonation also leads to reduction in the rate of rotation of heterocyclic rings. Figure 5a and b shows the ^1H NMR spectra of **10** at -50°C in its free base and protonated forms, respectively. Specifically, the free base of **10** shows the thiophene protons (t) at 0.55 and 0.35 ppm, with the bipyrrrole protons (bb', cc') at 8.93 and 8.36 ppm and the phenyl protons as a multiplet at 7.78 ppm. These assignments were made on the basis of the $^1\text{H}-^1\text{H}$ and $^1\text{H}-^{13}\text{C}$ COSY spectrum recorded at -50°C . The fact that the thiophene protons are still broad at this temperature suggests that the rotation is not completely arrested. Protonation of **10** leads to observance of reasonably resolved spectra at room

temperature (Figure 5c) and well-resolved spectra at -50°C (Figure 5b). The thiophene protons (t) experience a dramatic downfield shift (0.45 to 8.74 ppm) and the $-\text{NH}$ protons (e, d) appear as two singlets between -2 to -4 ppm. Furthermore, the bipyrrrole protons (bb', cc'), which were equivalent at room temperature, become inequivalent at -50°C , resulting in the appearance of an additional doublet of doublet (b, b', c, c'). Similar behavior is also observed for **17**.

In comparison, **11** behaved differently than **10**. The $^1\text{H}-^1\text{H}$ COSY spectrum recorded at -50°C is shown in Figure 6. In this case, it is possible to observe the inner $-\text{NH}$ proton as a broad signal at -1.0 ppm (d), and the selenophene protons appear at 9.85 ppm (a). Both the selenophene protons and the NH protons do not show any correlations, whereas the bipyrrrole protons (b, c) reveal correlation. Protonation of **11** leads to resolvable spectra at room temperature and well-resolved spectra at -50°C with sharp NH resonances, (Figure 5d and 5e). As in the case of **10**, here also the bipyrrrole protons (bb', cc') become inequivalent at -50°C . It was not possible to record

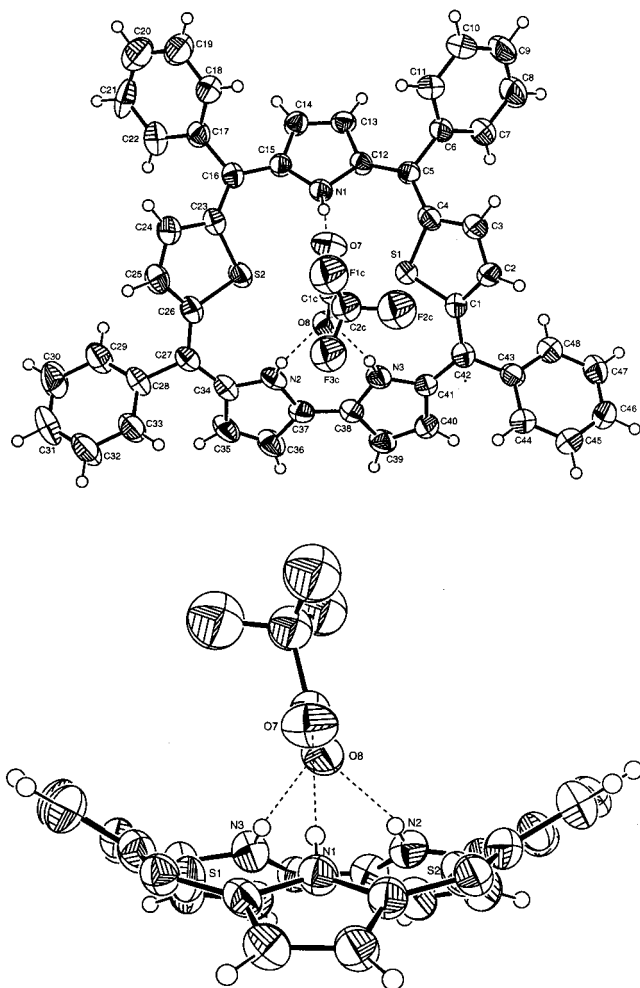


Figure 4. ORTEP diagram illustrating the geometry of the bound TFA anion in the complex [8.TFA]. Top, plane view; bottom, side view (phenyl rings are omitted for clarity). The other four TFA molecules (cocrystallized in the lattice) are also omitted for clarity.

well-resolved ^1H NMR spectra for the free base of **16** even at low temperature. However, the protonation leads to the same effects as observed for **10**, **11**, and **17**.

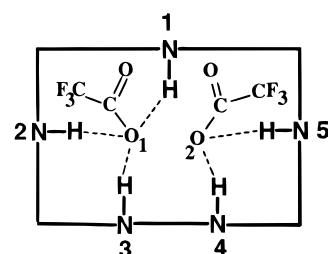
The conclusions arrived from ^1H NMR results on the solution structure of rubeirins are summarized in the Scheme 6. It is seen that **10** and **17** in their free base forms have similar structures in which both the thiophene rings in **10** and thiophene and furan rings in **17**⁴³ are inverted resulting in the appearance of β C–H ring protons in the shielded region as observed at -50°C . Protonation leads to the flipping of the thiophene rings, resulting in the appearance of these protons in the aromatic region. Such a ring inversion upon protonation has been observed by Latos-Grazynski et al.³⁹ for the N-5 *meso*-aryl sapphyrins, and to the best of our knowledge this is the first report on rubeirins. The solid-state structure of **10** (vide infra) also supports such an inversion of the thiophene rings. However, chemical shifts observed for the selenophene protons in the free base form for **11** force us to conclude that **11** has a normal structure at -50°C in which the two selenophene rings are not inverted in solution. However, the X-ray structure of **11** in its free base form in the solid state show inversion of the selenophene rings (vide infra). The protonated form of **16** also has the similar structure as observed for **10**, **11**, and **17**.

X-ray Structure of Rubeirins. The single-crystal X-ray structure of **10** in its free base form is shown in Figure 7. There

(43) Preliminary X-ray structure of **17** suggests that the furan and the thiophene rings are inverted in the solid state.

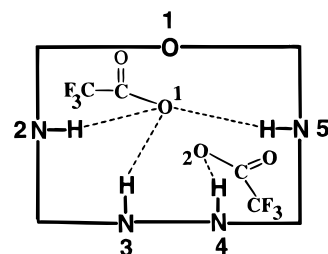
Scheme 5. Binding Modes of Trifluoroacetic Acid Anion to the N5 Sapphyrin, ON4 Sapphyrin, and S₂N₃ Sapphyrin **8**^a

N5-Sapphyrin



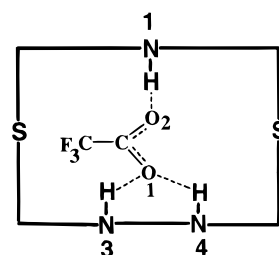
N1—H·····O1	2.913(7) Å
N2—H·····O1	2.927(7) Å
N3—H·····O1	2.921(7) Å
N4—H·····O2	2.781(7) Å
N5—H·····O2	2.899(7) Å

ON4-Sapphyrin



N2—H·····O1	2.830(3) Å
N3—H·····O1	2.967(3) Å
N5—H·····O1	2.910(4) Å
N4—H·····O2	2.847(4) Å

Sapphyrin-8



N1—H·····O2	2.807(7) Å
N3—H·····O1	2.804(8) Å
N4—H·····O1	2.790(1) Å

^a Data for N5 Sapphyrin and ON4 Sapphyrin are taken from ref 23(d).

are two molecules of benzonitrile solvent per macrocycle unit. It is clear from the figure that the two thiophene rings are inverted with respect to the plane containing the bipyrrrole rings. Specifically, the thiophene ring (S1) is 14.10° above and the thiophene ring (S1') is 14.10° below the plane containing the bipyrrroles. Substitution of pyrrole NH by thiophene S changes the π -electron delocalization, and the bond distances are altered accordingly relative to those observed for the HCl salt of N6 rubeirins¹⁶ (Table 2). The aromatic nature of the macrocycle is evident from the observation that the C_α – C_β distances (1.411(3) Å, 1.401(3) Å) are higher than the average C_β – C_β distances (1.360(3) Å).¹⁶ Furthermore, a comparison of the interpyrrole (heterocycle) angles at the bridging methines with

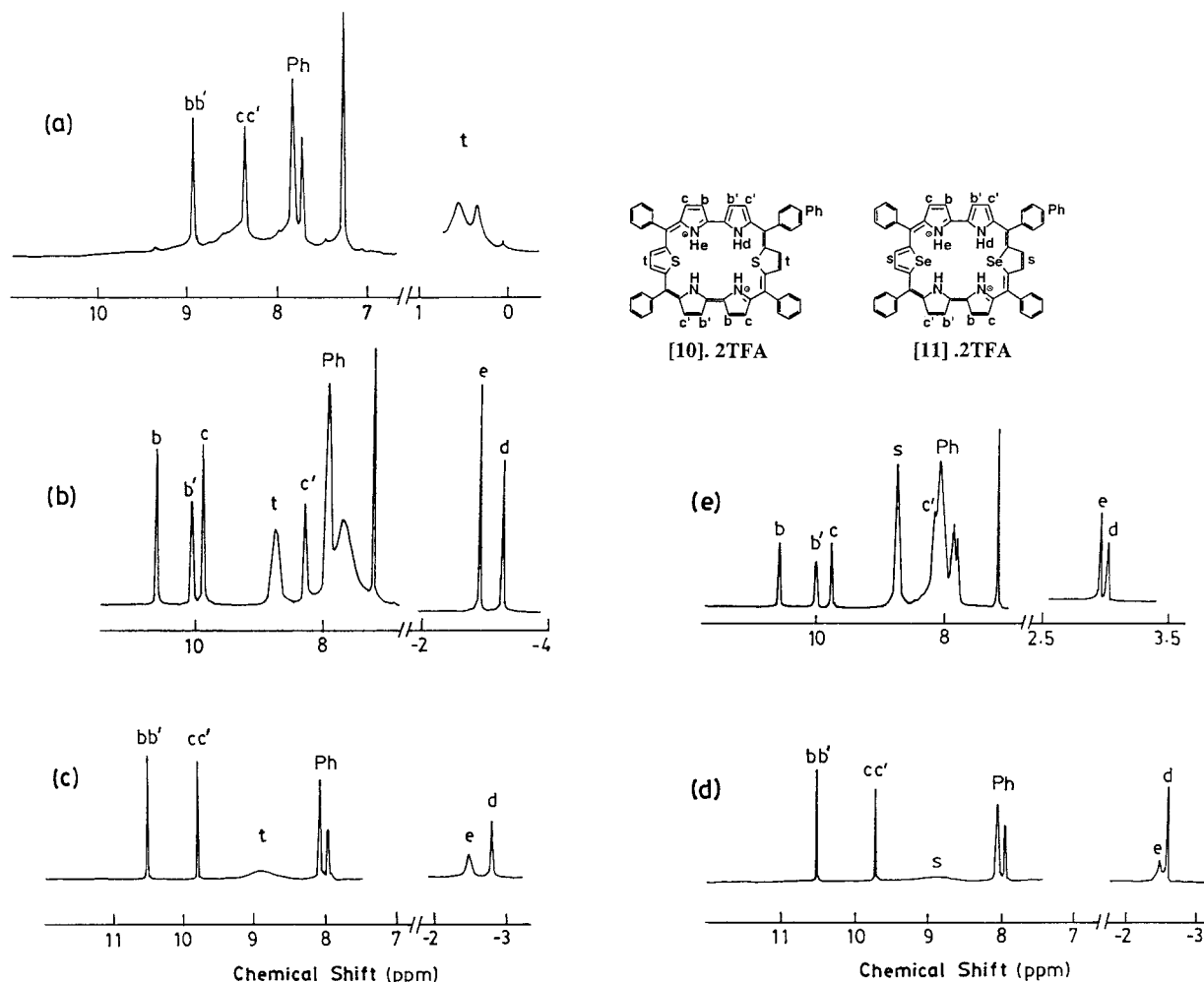


Figure 5. ^1H NMR (CDCl_3) spectra of (a) **10** at $-50\text{ }^\circ\text{C}$, (b) bis-TFA salt of **10** at $-50\text{ }^\circ\text{C}$, (c) bis-TFA salt of **10** at $25\text{ }^\circ\text{C}$, (d) bis-TFA salt of **11** at $25\text{ }^\circ\text{C}$, and (e) bis-TFA salt of **11** at $-50\text{ }^\circ\text{C}$.

those of the N6 rubyrins reveal significant lowering of the angles in **10**. For example, the angles C19–C12–C4 ($123.3(2)^\circ$) and C1–C5–C26' ($123.30(19)^\circ$) observed for **10** are lower than the corresponding angles observed for N6 rubyrins¹⁶ (137.0° and 137.63° , respectively), and surprisingly these angles are closer to that observed for porphyrins (127° for $\text{H}_2\text{OEP}^{2+}$),¹⁶ suggesting that the ring inversion results in the less open inner core. The repulsion due to the NH and CH are avoided by tilting of thiophene rings above and below the plane containing the bipyrrole.

The effect of ring inversion leads to increases (N2–N2' 7.431 Å for **8**, 6.345 Å for N6 rubyrin) in the distances of diagonal nitrogens and decreases (N1–N2 2.688 Å for **8**, 3.078 Å for N6 rubyrin) in the adjacent nitrogens relative to N6 rubyrins.¹⁶ The observed average C–N distances (1.359 Å) compares well with those observed for N6 rubyrins (1.365 Å).¹⁶ The C–S distances (1.745 Å) are close to the value observed for thia porphyrins (1.737 Å).⁴⁴

The single-crystal X-ray structure of **11** is shown in Figure 8. The unit cell contains two crystallographically independent molecules with a molecule of methanol coordinated to one of them. There are five nitrobenzene solvent molecules, one of which is highly disordered. The selenophene rings are found to be inverted, and both of the selenophene rings are above the mean plane defined by four meso carbons. The angle between

the plane containing the selenophene ring (Se1) and the plane containing the pyrrole ring (N4) is 23.01° . The $\text{C}_\alpha\text{--C}_\beta$ distances of the selenophene rings vary in this case. For example, C3–C4 and C1–C2 distances are 1.381(14) and 1.390(13) Å, respectively. On the other hand, C29–C30 and C27–C28 distances of other selenophene ring are 1.409(14) and 1.414(14) Å, respectively. Even the $\text{C}_\beta\text{--C}_\beta$ distances of two selenophene rings are different (C2–C3, 1.412(13) Å and C28–C29, 1.366(14) Å.) However, the $\text{C}_\alpha\text{--C}_\beta$ distances (C12–C13, 1.445(14) Å; C14–C15, 1.432(15) Å; C16–C17, 1.403(14) Å; C18–C19, 1.426(15) Å) are higher than the $\text{C}_\beta\text{--C}_\beta$ distances (C13–C14, 1.3119(15) Å; C17–C18, 1.381(15) Å), confirming the aromatic nature. The interpyrrole (heterocycle) angles at the bridging methines are $124.5(9)^\circ$ and $122.3(9)^\circ$, which are similar to those observed for **10**. Here also the ring inversion leads to increases in diagonal nitrogen distances (N1–N3, 7.323 Å) and decreases in adjacent nitrogen distances (N1–N2, 2.759 Å) relative to N6 rubyrins.¹⁶ The average C–N distance is 1.363 Å, and the C–Se distances (C1–Se1, 1.891(10) Å; C27–Se2, 1.903(11) Å) are closer to that observed for the selenaporphyrins (1.85 Å).^{26b, 45}

A comparison of the structures of **10** and **11** shows some similarities and some differences. In both structures the imino hydrogen atom could not be assigned unequivocally to a specific bipyrrole nitrogen atom as a result of the rapid interconversion

(44) Latos-Grazynski, L.; Lisowski, L.; Szterenber, L.; Olmstead, M. M.; Balch, A. L. *J. Org. Chem.* **1991**, *56*, 4043–4045.

(45) Latos-Grazynski, L.; Pacholska, E.; Chmielewski, P. J.; Olmstead, M. M.; Balch, A. L. *Inorg. Chem.* **1996**, *35*, 566–573.

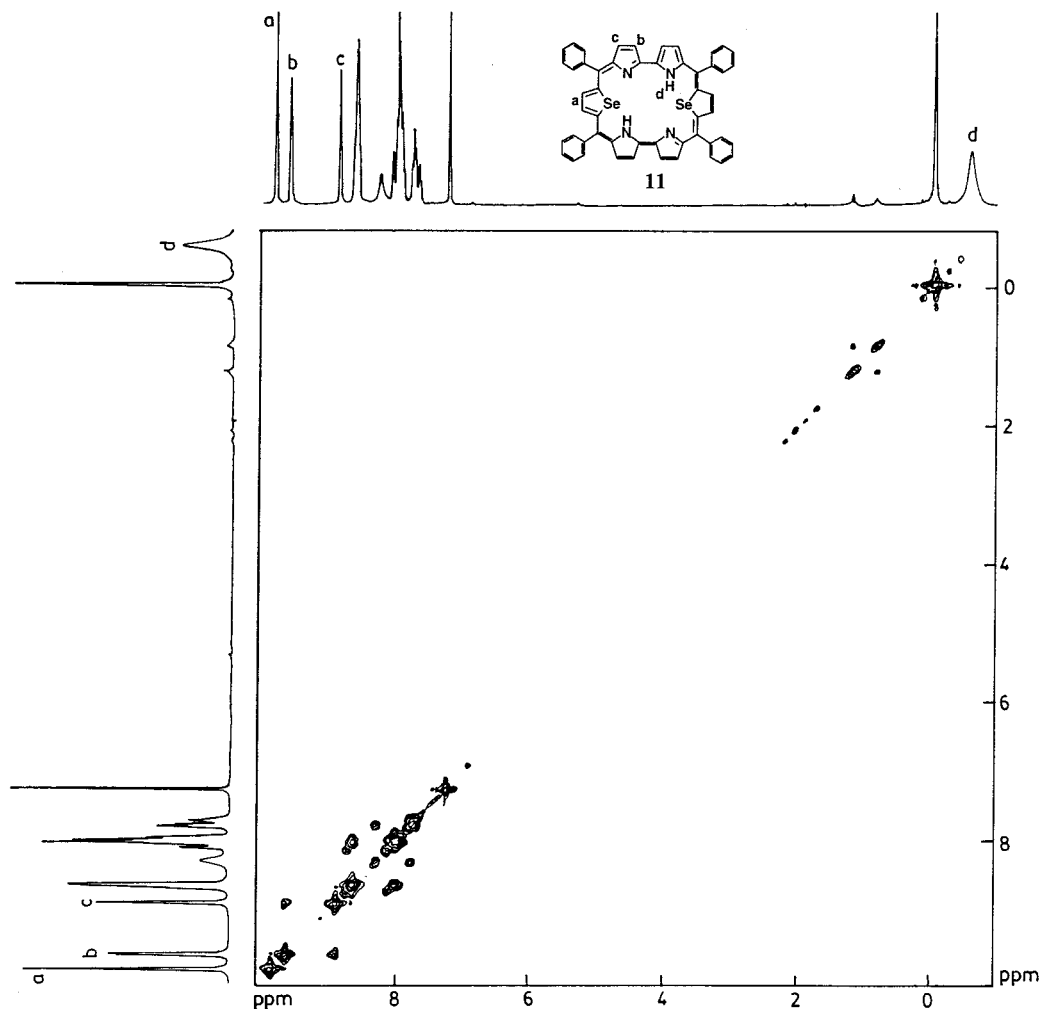
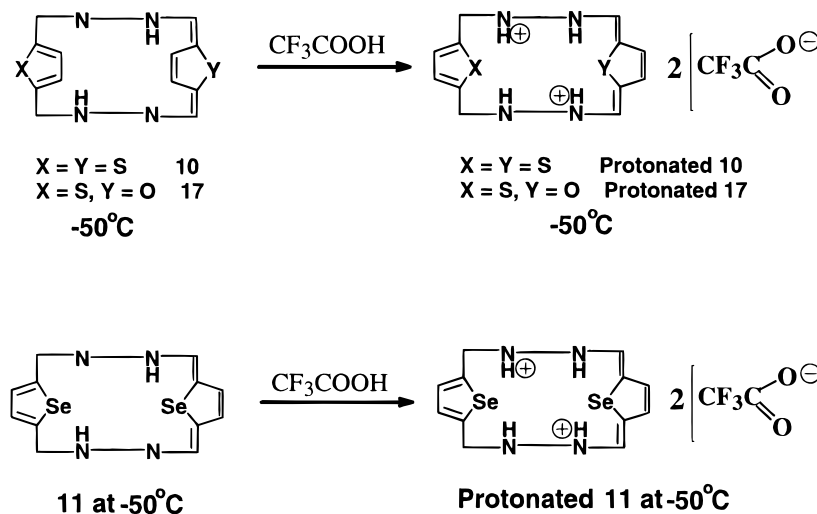


Figure 6. 2D ^1H - ^1H COSY spectra of **11** in CDCl_3 .

Scheme 6. Solution Structure of Rubyrins before and after Protonation



of NH tautomers during the time required for the measurement. Our analysis suggests a 50% probability of occupation on each nitrogen atom. The difference in the structure exists in the orientation of the inverted rings. For example, in **10** the thiophene rings are tilted above and below the plane containing bipyrrroles, thus making the β carbons C2 and C3 above the plane while C2' and C3' are below the plane by an angle of 14.10° . However, in **11**, both selenophene rings are above the plane containing the bipyrrrole units by an angle 23.01° , thus

making the β carbons C2, C3 and C28, C29 above the plane. This is clearly seen in the side view of Figures 7 and 8.

To get further insight into the inversion of the heterocyclic rings in rubyrin, the structure of selenatripyrrane **5** was solved by single-crystal X-ray diffraction (Figure 9). The structure clearly shows that the pyrrole rings are trans to each other with respect to the selenophene ring. The dihedral angles between the central selenophene and the terminal pyrroles (Se1-C1-C5-C12 and Se1-C4-C16-C23) are $31.3(6)^\circ$ and $65.7(5)^\circ$,

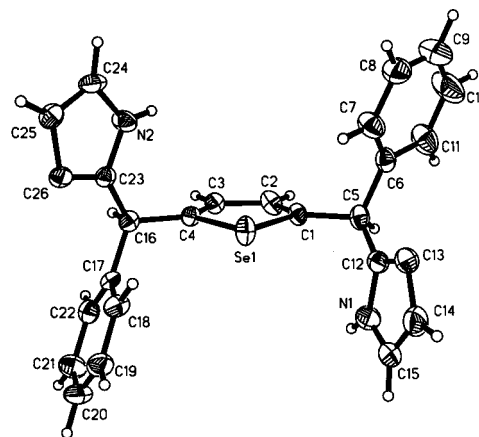
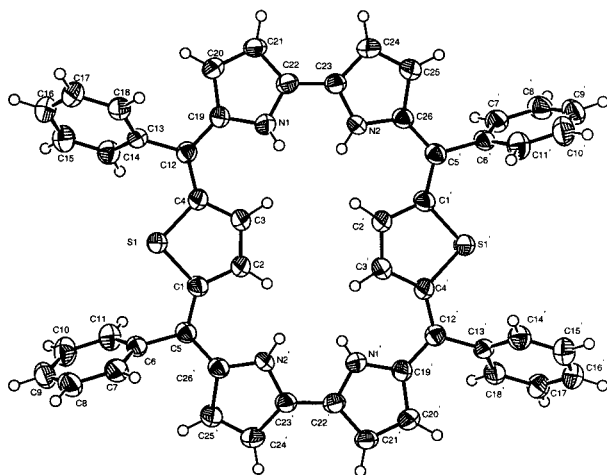


Figure 9. ORTEP diagram of the selenophene-containing tripyrrane **5**.

the required planar conformation for the formation of second pyrrole-pyrrole link is achieved through a possible free rotation along C1–C5 or C4–C16.^{29,34b}

Conclusions

Synthesis of a range of core-modified sapphyrins and rubyrins has been achieved by an acid-catalyzed condensation reaction involving a single precursor, the modified tripyrranes. The finding that the methodology works smoothly for three different tripyrranes and the possible cross-coupling reaction between two different tripyrranes highlights the versatility of the synthetic method. Successful synthesis of stable smaragdyrin, a new mode of binding of the TFA anion to the protonated sapphyrin, and the retention of a supramolecular array of sapphyrins in solution are some of the new features observed. Furthermore, the ring inversion of rubyrins in the solid state and the dramatic ring flipping on protonation are observed for the first time. It is hoped that the availability of easy synthetic methodologies to prepare these fascinating expanded porphyrins in multigram quantities will allow development of their diverse chemistry and the exploitation of their use in biomedical applications.

Experimental Section

Instrumentation. ¹H NMR spectra were measured on a 300 or 500 MHz Bruker spectrometer or a 400 MHz Varian spectrometer in CDCl₃ or CD₂Cl₂ solution. Chemical shifts are expressed in parts per million relative to residual CHCl₃ (7.258 ppm) or CH₂Cl₂ (5.3 ppm). FAB mass spectra were obtained on a JEOL SX-120/DA6000 spectrometer. The electrospray mass spectra were recorded on a MICROMASS QUATRO II triple quadrupole mass spectrometer. Analyses (C, H, N) were done on a Heraeus Carlo Erba 1108 elemental analyzer. The melting points are uncorrected and were measured on a JSGW melting point apparatus. The UV–vis spectra were recorded on a Shimadzu UV–vis spectrophotometer and a Perkin-Elmer Lambda 20 UV–vis spectrophotometer.

Materials. All NMR solvents were used as received. Dichloromethane was dried by distillation under nitrogen by calcium hydride. Tetrahydrofuran (THF) was distilled from sodium/benzophenone under nitrogen. Triethylamine was dried over KOH pellets and distilled under vacuum. *n*-Hexane was distilled under nitrogen from sodium. Pyrrole, thiophene, and furan (Aldrich) were distilled and then used. Selenophene was used as received. *n*-BuLi, trifluoroacetic acid (TFA), *p*-toluenesulfonic acid, and *p*-chloranil (Fluka) were used as received. Silica gel

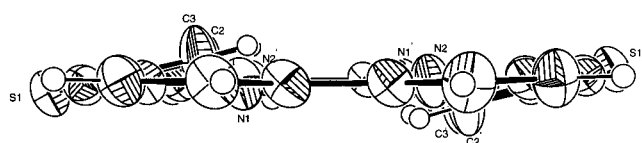


Figure 7. Two views of the molecular structure of **10** showing inverted thiophene rings. In the side view the phenyl rings are omitted for clarity.

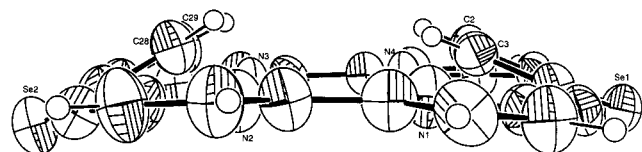
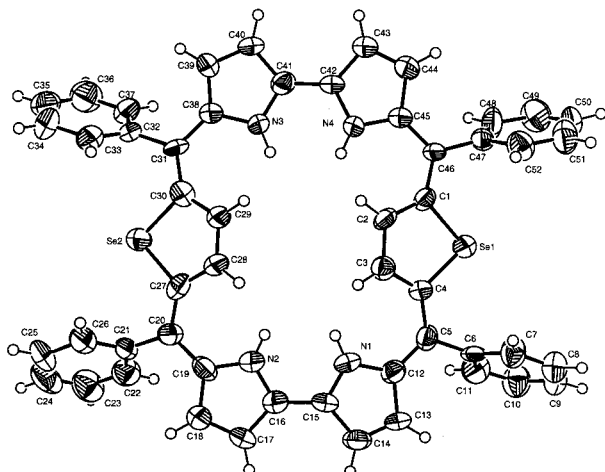


Figure 8. Two views of the molecular structure of **11** showing inverted selenophene rings. In the side view the phenyl rings are omitted for clarity.

respectively, thus showing that the molecule adopts a helical twist in the solid state.^{8d} This twisting of the molecule avoids the formation of linear polymeric products during the condensation process, thus supporting the so-called helical effect involved in the formation of the macrocycles.⁴⁶ It is possible that the first pyrrole–pyrrole link is formed in this conformation and

(46) (a) Franck, B. *Angew. Chem., Int. Ed. Engl.* **1982**, *21*, 343–353. (b) Bringmann, G.; Franck, B. *Liebigs Ann. Chem.* **1982**, 1272–1279. (c) Tietze, L. F.; Geissler, H. *Angew. Chem., Int. Ed. Engl.* **1993**, *32*, 1040–1042. (d) Vogel, E.; Dorr, J.; Herrmann, A.; Lex, J.; Schmickler, H.; Walgenbach, P.; Gisselbrecht, J. P.; Gross, M. *Angew. Chem., Int. Ed. Engl.* **1993**, *32*, 1597–1600.

Table 1. Crystallographic Data for **10**, **11**, **5**, and the TFA Adduct of **8**

	TFA adduct of 8	10	11	5
solvent for crystallization	dichloromethane/TFA/methanol	benzonitrile/methanol	nitrobenzene/ethanol/methanol	dichloromethane/ <i>n</i> -heptane
empirical formula	C ₅₈ H ₃₆ F ₁₅ N ₃ O ₁₀ S ₂	C ₆₆ H ₄₄ N ₆ S ₂	C ₁₃₆ H ₉₉ N ₁₃ O ₁₁ Se ₄	C ₂₆ H ₂₀ N ₂ Se
temperature (K)	298(2)	213(2)	298(2)	213(2)
crystal system	triclinic	monoclinic	triclinic	monoclinic
space group	<i>P</i> 1	<i>C</i> 2/ <i>c</i>	<i>P</i> 1	<i>P</i> 2(1)/ <i>c</i>
volume (Å ³)	2812.42(10)	5047.2(2)	5645.58(14)	2097.58(7)
<i>a</i> (Å)	13.7165(3)	29.0002(6)	16.8453(3)	5.9753(1)
<i>b</i> (Å)	14.8857(2)	15.0991(4)	17.1105(2)	13.1916(2)
<i>c</i> (Å)	16.5289(4)	11.9801(3)	21.2573(3)	26.6852(6)
α (deg)	104.403(1)	90	91.248(1)	90
β (deg)	109.278(1)	105.816(1)	112.815(1)	94.272(1)
γ (deg)	107.093(1)	90	90.368(1)	90
<i>Z</i>	2	4	2	4
calcd density (mg/m ³)	1.516	1.297	1.416	1.391
reflections collected	9469	10690	19762	10698
unique	5680	3601	11511	3946
<i>R</i> (int)	0.0603	0.0701	0.0575	0.0649
<i>F</i> (000)	1304	2056	2460	896
limiting indices	−13 ≤ <i>h</i> ≤ 13 −8 ≤ <i>k</i> ≤ 14 −16 ≤ <i>l</i> ≤ 16	−32 ≤ <i>h</i> ≤ 32 −16 ≤ <i>k</i> ≤ 11 −13 ≤ <i>l</i> ≤ 13	−16 ≤ <i>h</i> ≤ 14 −17 ≤ <i>k</i> ≤ 17 −21 ≤ <i>l</i> ≤ 21	−7 ≤ <i>h</i> ≤ 5 −15 ≤ <i>k</i> ≤ 16 −28 ≤ <i>l</i> ≤ 32
goodness of fit (<i>F</i> ²)	1.197	1.045	1.107	1.181
final <i>R</i> indices [<i>I</i> > 2σ(<i>I</i>)]	<i>R</i> ₁ = 0.0739 <i>wR</i> ₂ = 0.1784	<i>R</i> ₁ = 0.0444 <i>wR</i> ₂ = 0.1132	<i>R</i> ₁ = 0.0768 <i>wR</i> ₂ = 0.2041	<i>R</i> ₁ = 0.0656 <i>wR</i> ₂ = 0.1250
<i>R</i> indices (all data)	<i>R</i> ₁ = 0.0931 <i>wR</i> ₂ = 0.1926	<i>R</i> ₁ = 0.0598 <i>wR</i> ₂ = 0.1211	<i>R</i> ₁ = 0.1164 <i>wR</i> ₂ = 0.2207	<i>R</i> ₁ = 0.1042 <i>wR</i> ₂ = 0.1458

Table 2. Selected Bond Lengths (Å), Bond Angles (deg), and Torsional Angles (deg) for **10**, **11**, and **5**

	10	11	5
S1–C1	1.736(2)	Se1–C1	1.891(10)
S1–C4	1.753(2)	Se1–C4	1.887(10)
C1–C2	1.411(3)	C1–C2	1.390(13)
C2–C3	1.360(3)	C2–C3	1.412(13)
C3–C4	1.401(3)	C3–C4	1.381(14)
C1–C5	1.415(3)	C4–C5	1.404(14)
C4–C12	1.409(3)	C1–C46	1.411(13)
C5–C26'	1.408(3)	C5–C12	1.397(14)
C12–C19	1.420(3)	C46–C45	1.391(13)
C5–C6	1.496(3)	C5–C6	1.532(14)
C12–C13	1.488(3)	C46–C47	1.483(14)
N1–C19	1.364(3)	N1–C12	1.376(13)
N1–C22	1.352(3)	N1–C15	1.321(13)
C19–C20	1.427(3)	C12–C13	1.445(14)
C20–C21	1.372(3)	C13–C14	1.311(15)
C21–C22	1.414(3)	C14–C15	1.432(15)
C22–C23	1.416(3)	C15–C16	1.433(15)
		C41–C42	1.417(14)
N1–C3	2.90	N1–C3	2.935
N2'–N1	6.928	N1–N4	6.810
N1–N2	2.688	N1–N2	2.759
C3–C2'	4.248	C3–C28	4.780
N2–N2'	7.431	N1–N3	7.323
C1–S1–C4	93.49(10)	C1–Se1–C4	88.5(5)
C19–N1–C22	109.1(2)	C12–N1–C15	108.3(9)
S1–C4–C12	122.72(16)	Se1–C1–C46	122.2(8)
C3–C4–C12	128.98(10)	C2–C1–C46	128.6(9)
C4–C12–C19	123.3(2)	C4–C5–C12	124.5(9)
C20–C19–C12	129.2(3)	C13–C12–C5	129.1(10)
N1–C19–C12	123.39(19)	N1–C12–C5	124.4(10)
N1–C22–C23	118.33(10)	N1–C15–C16	119.0(10)
S1–C1–C5–C26'	−173.1(2)	Se1–C4–C5–C12	−169.2(9)
C1–C5–C6–C11	65.0(3)	C4–C5–C6–C7	64.9(14)
C4–C12–C19–C20	173.6(2)	C4–C5–C12–C13	−169.1(11)
N1–C22–C23–C24	179.7(2)	N1–C15–C16–C17	−179.3(12)
		C1–Se1–C4	87.8(2)
		C12–N1–C15	109.0(5)
		Se1–C1–C5	121.6(3)
		C2–C1–C5	128.4(4)
		C1–C5–C12	112.6(4)
		C13–C12–C5	132.1(5)
		N1–C12–C5	119.5(5)
		Se1–C1–C5–C12	31.3(6)
		C1–C5–C6–C7	59.2(6)
		C1–C5–C12–C13	−114.8(6)

(100–120 mesh) or basic alumina (Merck, usually Brockmann grade III) was used for column chromatography. 16-Thiatripyrrene (**4**) and 16-oxatripyrrene (**12**) were prepared according to the published procedure^{11c} and stored under inert atmosphere at −10 °C.

X-ray Structure Determinations. The trifluoroacetate salt of **8** was

obtained by stirring a chloroform solution containing 10% TFA and the recrystallized sample of free base **8**. The solution was evaporated, and the single crystal of **8.TFA** was obtained by layering the 10% TFA/dichloromethane solution of **8.TFA** with methanol in a thin glass tube. The same crystallization technique was used to obtain the single crystals

of **10**, **11**, and **5** using appropriate solvent mixtures as shown in the Table 1. The X-ray diffraction data were collected on a Siemens SMART 3-circle diffractometer equipped with a CCD detector. The data were acquired with the Siemens SMART software and processed on a SGI-Indy/Indigo 2 workstation by using the SAINT software. Graphite monochromated Mo K α radiation ($\lambda = 0.71073 \text{ \AA}$) was used for data collection. The structures were solved by direct methods using the SHELXS 90 program and refined by full-matrix least squares on F² using SHELXL 93, incorporated in SHELXTL-PC V 5.03. Details of crystals are listed in Table 1 and selected bond lengths and angles are given in Table 2. Other pertinent information, including X-ray experimental details for each compound, is included in the Supporting Information.

Syntheses. 2,5-Bis(phenylhydroxymethyl)selenophene. A 2,5-dilithioselenophene suspension was prepared by adding butyllithium (12.72 mL, 19.08 mmol) at room temperature to a mixture of *n*-hexane (40 mL), TMEDA (2.87 mL, 19.08 mmol), and selenophene (1 g, 7.60 mmol) in an inert atmosphere. The mixture was stirred for about 30 min and then refluxed for 1 h to complete the conversion. Then the mixture was allowed to cool to 10 °C, and benzaldehyde (1.93 mL, 19.08 mmol) in dry THF (15 mL) was added dropwise. The temperature of the reaction mixture was gradually raised to room temperature, and stirring was continued for 60 min. The reaction was quenched with saturated ammonium chloride solution and stirred for 30 min. The organic layer was separated, and the aqueous layer was extracted with diethyl ether. The organic layers were combined and dried over sodium sulfate. The solvent was evaporated, and the product was recrystallized from toluene to afford a white solid (yield 1.59 g, 57%): mp 143–144 °C; ¹H NMR (400 MHz, CDCl₃) δ 2.27(br s, 2H), 5.85(s, 2H), 6.77(s, 2H), 7.17–7.28(m, 6H), 7.30–7.38(m, 4H); EI-MS 343 (M⁺). Anal. Calcd for C₁₈H₁₆O₂Se: C, 62.98; H, 4.70. Found: C, 62.92; H, 4.73.

16-Selenatripyrrane (5). 2,5-Bis(phenylhydroxymethyl)selenophene (0.7 g, 2.04 mmol) was dissolved in pyrrole (5.6 mL, 81.60 mmol), and the mixture was degassed by bubbling nitrogen gas. Trifluoroacetic acid (TFA) (0.015 mL, 0.20 mmol) was added to this solution, and the mixture was stirred for about 30 min at room temperature. The completion of the reaction was followed with TLC. Dichloromethane (100 mL) was added, and the reaction mixture was neutralized with 40% NaOH solution. The organic layer was separated and washed two times with water (50 mL) before drying over sodium sulfate. The excess pyrrole was removed at room temperature by vacuum. Chromatography on silica gel with ethyl acetate and petroleum ether (1:10) gave the desired tripyrrane as a pale yellow solid (yield 0.65 g, 75%): mp 105–106 °C; ¹H NMR (300 MHz, CDCl₃) δ 5.59(s, 2H), 5.97(s, 2H), 6.16–6.13(m, 2H), 6.68(m, 2H), 6.80(s, 2H), 7.35–7.24(m, 10H), 7.91(br s, 2H); EI-MS: 443 (M⁺). Anal. Calcd for C₂₆H₂₄N₂Se: C, 70.42; H, 5.45; N, 6.32. Found: C, 70.47; H, 5.48; N, 6.28.

General Procedure for the Synthesis of Macrocycles. 5,10,15,20-Tetraphenyl-26,28-dithiasapphyrin (8) and 5,10,19,24-Tetraphenyl-30,33-dithiarubyrin (10). 16-Thiatripyrrane **4** (0.12 g, 0.301 mmol) dissolved in dry CH₂Cl₂ (150 mL) was stirred under nitrogen atmosphere for 5 min. The reaction mixture was protected from sunlight. TFA (0.023 mL, 0.301 mmol) was added, and stirring was continued for a further 90 min. Chloranil (0.22 g, 0.903 mmol) was added, and the reaction mixture was opened to air and refluxed for further 90 min. The mixture was neutralized with triethylamine, and the solvent was evaporated in vacuo. The residue so obtained was chromatographed on a basic alumina column. The first orange fraction eluted with petroleum ether and dichloromethane (2:1) gave a purple solid identified as dithiaporphyrin **6** (2 mg, 1%). The second green band eluted with ethyl acetate/dichloromethane (1:10) gave a greenish purple solid that was identified as 5,10,15,20-tetraphenyl-26,28-dithiasapphyrin **8** (yield 30 mg, 14%, recrystallized from toluene/*n*-heptane (1:1): decomposes above 280 °C; ¹H NMR (300 MHz, CDCl₃, 25 °C) δ 7.85(m, 7H), 7.92(m, 4H), 8.37(m, 4H), 8.46(m, 4H), 8.81(s, 2H), 9.29(d, 2H, *J* = 3 Hz), 9.93(d, 2H, *J* = 6 Hz), 9.95(d, 2H, *J* = 6 Hz), 10.06(d, 2H, *J* = 6 Hz); ¹H NMR (300 MHz, CDCl₃/TFA, 25 °C) δ -2.18(br s, 2H), -2.85(s, 1H), 8.18(m, 8H), 8.23(m, 4H), 8.76(m, 4H), 8.89 (m, 4H), 9.17(s, 2H), 9.75(d, 2H, *J* = 6 Hz), 10.12(d, 2H, *J* = 6 Hz), 10.32(d, 2H, *J* = 6 Hz), 10.33(d, 2H, *J* = 6 Hz); UV-vis (CH₂Cl₂) λ_{max} (nm)

($\epsilon \times 10^{-4}$) 470(22.4), 584(1.75), 623(1.07), 730(0.59), 820(1.68); UV-vis (CH₂Cl₂/TFA) λ_{max} (nm) ($\epsilon \times 10^{-4}$) 499(12.3), 660sh (1.17), 727-(2.42), 826(2.74); FAB-MS *m/z* 714 [M⁺]. Anal Calcd for C₄₈H₃₁N₃S₂: C, 80.76; H, 4.38; N, 5.89. Found: C, 80.80; H, 4.35; N, 5.86. The last pink band eluted with ethyl acetate/dichloromethane (1:3) gave a lustrous green solid, identified as the 5,10,19,24-tetraphenyl-30,33-dithiarubyrin **10** (yield 20 mg, 8.5%, recrystallized from dichloromethane/*n*-heptane (1:1): decomposes above 300 °C; ¹H NMR (500 MHz, CDCl₃, -50 °C) δ 0.35(s, 2H), 0.55(s, 2H), 7.45–7.48(m, 8H), 7.73–7.74(m, 12H), 8.360(s, 4H), 8.932(s, 4H); ¹H NMR (300 MHz, CDCl₃/TFA, -50 °C) δ -2.91(s, 2H), -3.28(s, 2H), 7.68–7.94(m, 20H), 8.28(d, *J* = 6 Hz, 2H), 8.74(br s, 4H), 9.89(d, *J* = 6 Hz, 2H), 10.06(d, *J* = 6 Hz, 2H), 10.62(d, *J* = 6 Hz, 2H); ¹H NMR (500 MHz, CDCl₃/TFA, 25 °C) δ -2.47(br s, 2H), -2.80(s, 2H), 7.95–7.98(m, 8H), 8.09(m, 12H), 8.88(br s, 4H), 9.80(d, *J* = 4 Hz, 4H), 10.54(d, *J* = 4 Hz, 4H); UV-vis (CH₂Cl₂) λ_{max} (nm) ($\epsilon \times 10^{-4}$) 385(0.16), 532(14.2), 658(1.12), 764(0.9), 1017(1.36); UV-vis (CH₂Cl₂/TFA) λ_{max} (nm) ($\epsilon \times 10^{-4}$) 542(19.4), 722(0.82), 813(1.8), 1004 (5.9); FAB-MS *m/z* 779 [M⁺]. Anal Calcd for C₅₂H₃₄N₄S₂: C, 80.18; H, 4.40; N, 7.19. Found: C, 80.16; H, 4.35; N, 7.22.

5,10,15,20-Tetraphenyl-26,28-diselenasapphyrin (9) and 5,10,19,24-Tetraphenyl-30,33-diselenarubyrin (11). The above procedure was followed using the 16-selenatripyrrane **5** (0.15 g, 0.34 mmol), TFA (0.053 mL, 0.68 mmol), and chloranil (0.25 g, 1.03 mmol). Sapphyrin **9** as a greenish purple solid and rubyrin **11** as a green solid were obtained in 9.2% (25.4 mg) and 18.3% (54.6 mg) yields, respectively. Data for **9**: decomposes above 280 °C; ¹H NMR (300 MHz, CDCl₃, 25 °C) δ -4.4(br s, 1H), 7.6(m, 8H), 7.96(m, 4H), 8.39(m, 4H), 8.49 (m, 4H), 8.96(s, 2H), 9.36(d, 2H, *J* = 6 Hz), 10.01(d, 2H, *J* = 6 Hz), 10.35(d, 2H, *J* = 6 Hz), 10.47(d, 2H, *J* = 6 Hz); UV-vis (CH₂Cl₂) λ_{max} (nm) ($\epsilon \times 10^{-4}$) 475(30.1), 517(6.4), 592(2.8), 631(1.8), 736-(0.7), 823(3.2); UV-vis (CH₂Cl₂/TFA) λ_{max} (nm) ($\epsilon \times 10^{-4}$) 519-(19.8), 677 (0.96), 752 (1.83), 859(2.9); FAB-MS *m/z* 810 [M⁺ for 80Se]. Anal Calcd for C₄₈H₃₁N₃Se₂: C, 71.38; H, 3.87; N, 5.20. Found: C, 71.32; H, 3.89; N, 5.25. Data for **11**: decomposes above 300 °C; ¹H NMR (300 MHz, CDCl₃, -50 °C) δ 9.88(s, 4H), 9.66(d, 4H, *J* = 4.2 Hz), 8.91(d, 4H, *J* = 4.2 Hz), 8.64–8.66(m, 8H), 7.94–8.10(m, 8H), 7.68–7.81(m, 4H), -0.06(br, s); ¹H NMR (300 MHz, CDCl₃/TFA, -50 °C) δ -2.95(s, 2H), -3.07(s, 2H), 7.87–8.15(m, 20H), 8.24(d, *J* = 6 Hz, 2H), 8.82(br s, 4H), 9.83(d, *J* = 6 Hz, 2H), 10.06(d, *J* = 6 Hz, 2H), 10.62(d, *J* = 6 Hz, 2H); ¹H NMR (500 MHz, CDCl₃/TFA, 25 °C) δ -2.47(br s, 2H), -2.56(br s, 2H), 7.94–7.97(m, 8H), 8.06-(m, 12H), 8.9(br s, 4H), 9.72(d, *J* = 4 Hz, 4H), 10.53(d, *J* = 4 Hz, 4H); UV-vis (CH₂Cl₂) λ_{max} (nm) ($\epsilon \times 10^{-4}$) 530(13.4), 666(1.09), 766(0.62), 849(0.77), 970(1.34); UV-vis (CH₂Cl₂/TFA) λ_{max} (nm) ($\epsilon \times 10^{-4}$) 546 (15.4), 728 (0.98), 814(1.11), 1016(5.07); FAB-MS *m/z* 875(100) [M⁺ for 80Se]. Anal Calcd for C₅₂H₃₄N₄Se₂: C, 71.56; H, 3.93; N, 6.42. Found: C, 71.52; H, 3.96; N, 6.43.

5,10,19-Tetraphenyl-25-oxasamaragdyrin (13). This was prepared by the reaction of 16-oxatripyrrane **12** (0.15gm, 0.4 mmol) with TFA (0.003 mL, 0.042 mmol) followed by oxidation with chloranil (0.29gm, 1.19 mmol) by a similar procedure as described above. The crude product upon chromatographic separation on basic alumina with petroleum ether and dichloromethane (3:10) gave **13** as a purple solid (yield 7.8 mg, 3.3%): decomposes above 275 °C; ¹H NMR (300 MHz, CDCl₃, 25 °C) δ 7.83(m, 9H), 8.21(m, 4H), 8.38(m, 2H), 8.42(d, *J* = 4.2 Hz, 2H), 8.74(s, 2H), 8.95(d, *J* = 4.2 Hz, 2H), 9.36(d, *J* = 4.2 Hz, 2H), 9.46 (d, *J* = 4.2 Hz, 2H); UV-vis (CH₂Cl₂) λ_{max} (nm) ($\epsilon \times 10^{-4}$) 443(33.0), 456sh (16.0), 552(2.0), 591(1.4), 633(1.0), 696(1.4); UV-vis (CH₂Cl₂/HCl) λ_{max} (nm) ($\epsilon \times 10^{-4}$) 450(27.9), 482(13.5), 605(1.8), 657(2.4), 720(4.6); emission (CH₂Cl₂) $\lambda = 701 \text{ nm}$; FAB-MS *m/z* 593 [M⁺]. Anal Calcd for C₄₁H₂₈N₄O: C, 83.09; H, 4.76; N, 9.45. Found: C, 83.14; H, 4.72; N, 9.49.

5,10,15-Tetraphenyl-21-oxacorrole (14). This was prepared by a similar procedure as above with 16-oxatripyrrane **12** (0.167gm, 0.44 mmol), TFA (0.17 mL, 2.2 mmol), and chloranil (0.328 mg, 1.33 mmol). In the chromatographic separation on basic alumina, the first band eluted with a mixture of petroleum ether and dichloromethane (1:10) gave **14** as a purple solid (yield 10 mg, 4.3%): decomposes above 270 °C; ¹H NMR (300 MHz, CDCl₃, 25 °C) δ -1.91(s, 1H), 7.77(m, 9H), 8.13 (m, 2H), 8.30(m, 4H), 8.35(d, 1H, *J* = 4.5 Hz),

8.57(q, 1H), 8.78(d, 1H, $J = 5.1$ Hz), 8.80 (d, 1H, $J = 4.8$ Hz), 8.82-(d, 1H, $J = 4.2$ Hz), 9.03(d, 1H, $J = 4.2$ Hz), 9.05(q, 1H), 9.09(d, 1H, $J = 5.1$ Hz); UV-vis (CH_2Cl_2) λ_{max} (nm) ($\epsilon \times 10^{-4}$) 411(27.0), 497-(1.6), 528(1.6), 583 (0.7), 632 nm (2.1); UV-vis ($\text{CH}_2\text{Cl}_2/\text{HCl}$) λ_{max} (nm) ($\epsilon \times 10^{-4}$) 412(24.3), 431sh (13.7), 523(3.2), 583(0.3), 635(5.4); emission (CH_2Cl_2) $\lambda = 640$ nm; emission ($\text{CH}_2\text{Cl}_2/\text{HCl}$) $\lambda = 652$ nm; FAB-MS m/z 528 [M^+]. Anal Calcd for $\text{C}_{37}\text{H}_{25}\text{N}_3\text{O}$: C, 84.23; H, 4.78; N, 7.96. Found: C, 84.27; 4.75; N, 7.99.

5,10,15,20-Tetraphenyl-26,28-dioxasapphyrin (15) and 5,10,19,24-Tetraphenyl-30, 33-dioxarubyrin (16). These compounds were prepared similarly as above from 16-oxatripyrrane **12** (0.18 g, 0.47 mmol), TFA (0.07 mL, 0.93 mmol), and chloranil (0.34 g, 1.40 mmol). Chromatographic separation on basic alumina with ethyl acetate/dichloromethane (1:1) gave **15** as a greenish purple solid (yield 7.1 mg, 2.3%). Upon changing the eluent to a mixture of dichloromethane/methanol (1:1) **16** came as a greenish brown solid (yield 54 mg, 15.6%). Data for **15**: decomposes above 270 °C; ^1H NMR (300 MHz, CDCl_3) δ -0.75 (s, 2H), 7.66 (m, 4H), 7.85 (m, 8H), 8.31 (m, 4H), 8.78 (d, 4H), 8.89(d, $J = 6$ Hz, 2H), 9.12 (d, $J = 6$ Hz, 2H), 9.54 (d, $J = 6$ Hz, 2H), 9.74 (d, $J = 6$ Hz, 2H); UV-vis (CH_2Cl_2) λ_{max} (nm) ($\epsilon \times 10^{-4}$) 474(20.11), 581(2.1), 625(1.79), 741(0.59), 838(1.36); UV-vis ($\text{CH}_2\text{Cl}_2/\text{TFA}$) λ_{max} (nm) ($\epsilon \times 10^{-4}$) 476 (16.0), 504(9.2), 629 (1.30), 686-(1.11), 806(2.3); FAB-MS m/z 683 [$\text{M} + 1$]. Anal Calcd for $\text{C}_{48}\text{H}_{31}\text{N}_3\text{O}_2$: C, 84.56; H, 4.58; N, 6.16. Found: C, 84.54; H, 4.59; N, 6.19. Data for **16**: decomposes above 300 °C; ^1H NMR (300 MHz, CDCl_3/HCl , 25 °C) δ -1.55(br s, 2H), -1.6(br s, 2H), 7.98(m, 12H), 8.51(s, 4H), 8.77(m, 8H), 9.61(s, 4H), 9.86(s, 4H); UV-vis (CH_2Cl_2) λ_{max} (nm) ($\epsilon \times 10^{-4}$) 564(4.8), 703(0.7), 771(1.26), 900(0.39), 1041-(2.22); UV-vis ($\text{CH}_2\text{Cl}_2/\text{TFA}$) λ_{max} (nm) ($\epsilon \times 10^{-4}$) 524(8.3), 584-(2.8), 720(0.3), 875 (0.21), 985(2.46); FAB-MS m/z 748 [$\text{M} + 1$]. Anal Calcd for $\text{C}_{52}\text{H}_{34}\text{N}_4\text{O}_2$: C, 83.63; H, 4.59; N, 7.50. Found: C, 83.68; H, 4.63; N, 7.46.

5,10,19,24-Tetraphenyl-30-thia-33-oxarubyrin (17). This was synthesized by the reaction of 16-thiatripyrrane **4** (0.32gm, 0.82 mmol) and 16-oxatripyrrane **12** (0.31gm, 0.82 mmol) with TFA (0.006 mL, 0.08 mmol) followed by chloranil (0.61gm, 2.47 mmol) oxidation. This was purified from column chromatography (basic alumina). Elution with 1:10 ethyl acetate/dichloromethane gave **10** (20 mg, 2.8%). A pink band eluted with mixture of 2:10 ethyl acetate/dichloromethane gave a green solid identified as **17** (yield 160 mg, 25%): decomposes above

300 °C; ^1H NMR (300 MHz, CDCl_3 , -50 °C) δ 2.15(s, 2H), 2.69(s, 2H), 7.47-7.52(m, 8H), 7.66-7.70(m, 12H), 8.09-8.10(d, 1H), 8.15-(s, 1H), 8.18(s, 1H), 8.19(s, 1H), 8.23(s, 1H), 8.26(s, 1H), 8.45-8.46-(d, 1H), 8.48-8.50(d, 1H); ^1H NMR (300 MHz, CDCl_3/TFA , -50 °C) δ -1.83(s, 1H), -2.06(s, 1H), -2.21(s, 1H), -2.32(s, 1H), 7.80-7.85-(m, 8H), 7.94(br s, 2H), 8.05-8.10(m, 12H), 8.21(d, 1H), 8.25(s, 1H), 8.73(br s, 2H), 8.86(d, $J = 6$ Hz, 1H), 9.70(d, $J = 6$ Hz, 1H), 9.80(d, $J = 6$ Hz, 1H), 9.84(s, 1H), 10.30(d, $J = 6$ Hz, 1H), 10.34(d, $J = 6$ Hz, 1H); ^1H NMR (500 MHz, CDCl_3/TFA , 25 °C) δ -1.48(s, 1H), -1.77(s, 1H), -1.84(s, 1H), -1.94(s, 1H), 7.80-7.83(m, 4H), 7.94-7.97(m, 4H), 8.02-8.09(m, 12H), 8.81(s, 2H), 8.82(s, 2H), 9.63(d, $J = 4$ Hz, 2H), 9.75(d, $J = 4$ Hz, 2H), 10.24(d, $J = 4$ Hz, 2H), 10.28(d, $J = 4$ Hz, 2H); UV-vis (CH_2Cl_2) λ_{max} (nm) ($\epsilon \times 10^{-4}$) 530(17.3), 647(2.0), 772(0.6), 1015(2.1); UV-vis ($\text{CH}_2\text{Cl}_2/\text{TFA}$) λ_{max} (nm) ($\epsilon \times 10^{-4}$) 549(34.7), 723(1.48), 807(1.4), 1011(10.9); electrospray-MS m/z 763 [M^+]. Anal Calcd for $\text{C}_{52}\text{H}_{34}\text{N}_3\text{SO}$: C, 81.87; H, 4.49; N, 7.34. Found: C, 81.88; H, 4.46; N, 7.38.

Acknowledgment. This work was supported by a grant from the Department of Science & Technology (DST) and Council of Scientific and Industrial Research (CSIR), Government of India, New Delhi, to T.K.C. The single-crystal CCD X-ray facility at the University of Idaho was established with the assistance of the NSF-Idaho EPSCoR program under NSF OSR-9350539 and the M.J. Murdock Charitable Trust, Vancouver, WA. The use of the 500 MHz NMR spectrometer at TIFR, Bombay, is acknowledged. This paper is dedicated to Professor P. T. Manoharan on the occasion of his 64th birthday.

Supporting Information Available: 1D and 2D NMR spectra of compounds **5**, **8-11**, **13-15**, and **17**, along with tables of crystal data, structure solution and refinement, atomic coordinates, bond lengths and angles, and anisotropic thermal parameters for compounds **5**, **10**, **11**, and the TFA adduct of **8**. X-ray crystallographic files are available through the Web only. This material is available free of charge via the Internet at <http://pubs.acs.org>.

JA991472K